'Compuscript edited Dec. 02'

Development of the Application of Speciation in Chemistry

Tamás Kiss [a,b,*], Éva A. Enyedy [a], Tamás Jakusch [a]

[a] Department of Inorganic and Analytical Chemistry, University of Szeged, Dóm tér 7, H-6720 Szeged, Hungary

[b] MTA-SZTE Bioinorganic Chemistry Research Group, University of Szeged, Dóm tér 7, H-6720 Szeged, Hungary

Contents

* Corresponding author. Tel.: +36/36-62-544-337
E-mail address: tkiss@chem.u-szeged.hu

Abstract

This review provides definitions and examples of chemical speciation, as well as giving details of the differences in speciation between labile and inert systems. By moving from the simple to the complex, starting with simple species distribution calculation methods based on solution structural studies, this review progresses to modeling calculations that are applicable to “real-world” systems. The biological and or medicinal speciation of the following metal ions are discussed (modeling and experimental confirmation of the calculation results as well as kinetic aspects of their changes in speciation): Al(III), Fe(III), Ga(III), Gd(III), Ru(III), Ca(II), Cu(II), Pd(II), V(IV)O, V(V), and Zn(II)). Brief introductions are also given to trace analytical and environmental speciation. The current status and future possibilities of speciation studies (evaluation and prediction of speciation data), data collection, and databases are also critically discussed.

Keywords: biospeciation, equilibrium model, human serum, kinetic aspect of speciation, modeling calculation, spectroscopy

1. Definitions of speciation and fractionation

The term “speciation” is generally used to indicate the analytical activity/concentration when identifying chemical species and to measure their distribution. Thus, speciation is used to describe the distribution of species in a particular sample, where it is synonymous with the “species distribution,” e.g., “the bioavailability of aluminum depends strongly on its speciation” [1]. An element may be present in different chemical forms in terms of the isotopic composition, oxidation state, and type of binding ligand (solvent molecules, inorganic or organic small molecules, macromolecules, labile or inert bound ligands, etc.). For instance, as described in detail later, the hydrolysis of the Al(III) ion in equilibrium solution can yield numerous species depending on the pH and concentration, such as $[Al(OH)]^{2+}$, $[Al(OH)_2]^{+}$, $Al(OH)_3$, $[Al(OH)_4]^{-}$, $[Al_2(OH)_2]^{4+}$, $[Al_3(OH)_4]^{5+}$, and the oligonuclear $[Al_{13}O_4(OH)_{24}]^{7+}$ [2], where thermodynamic equilibrium/formation constants characterize their stability in solution [3].

Another example is when the oxidation state of an element profoundly affects its toxicity. Thus, the more reduced species of As are the most toxic as follows: arsine (AsH_3) > arsenite (As(III)) > arsenate (As(V)) [4]. The oxidation state may also have a strong impact on the absorption and elimination features of a metal ion. The Fe(II) ion is soluble under physiological conditions and transported freely across membranes, whereas Fe(III) does not enter cells and is more prone to hydrolysis in biological systems [5]. The uptake of iron from Fe(III)-containing species probably involves decomposition, reduction, and transport into the cell in the form of Fe(II) [6]. It should be noted that iron is found in both Fe(II) and Fe(III) oxidation states in the human body, where the transport and storage processes often involve redox transformation of the metal ion.

It is often not possible to determine the concentrations of different chemical species that comprise the total concentration of an element in a given sample. For example, in many cases, the presence of a large number of individual species (e.g., in metal-humic acid complexes, metal-fulvic acid complexes, or metal complexes in biological fluids) can make it practically impossible to determine their speciation. In these cases, it may be useful to identify the various classes of species of an element in order to determine their summed concentration in each class [7]. This fractionation process can be based on many different properties of the chemical species, such as their size, molecular mass, solubility, charge, and affinity.

Fractionation may involve actual physical separation, e.g., filtration or size-exclusion chromatography. It is useful to measure the total concentration of the element in each fraction in order to verify the mass balance. In some situations, the fractions can be analyzed further for individual species based on subsequent analyses and calculations.

For instance, the total Al content of natural waters is not relevant to their harmful biological effects. However, Al(III) binds to inorganic ligands and low molecular mass (LMM) organic molecules to yield toxic forms of this metal ion. These forms are mobile and can be absorbed more easily by organisms, before being transported within biological systems to cause harmful biological effects. Metal ions bound to high molecular mass (HMM) bioligands are in a much more sluggish environment, so they are less able to react with endogenous molecules in biological fluids or cells.

It should be noted that all the basic definitions and technical terms used in this study regarding complex formation equilibria (such as component, binary complex, and conditional stability constant) were specified in previous studies [8-11].

2. Speciation in inert and labile chemical systems

2.1. Labile systems

In labile systems, all equilibria (at least one) are always reached. Fast equilibrium processes make it impossible to study the pure individual compounds in all conditions. One of the simplest examples is the dimerization equilibrium of nitrogen dioxide, where only N_2O_4 forms under normal pressure and at < 263 K, whereas the NO_2 form exists at > 413 K. The two species are inseparable at temperatures between these limits and an equilibrium state is always reached [12a]. An important characteristic of these labile systems is the equilibrium constant(s), which depends on various conditions, such as the temperature (T), pressure (p), solvent, and ionic strength (I). The classic example of a labile system comprises $3d^5$-$3d^{10}$ divalent transition metal ions, which form labile complexes, with a few rare exceptions. For example, these metal ions (M) form complexes with simple monodentate anions (L), such as halides and pseudohalides, with different compositions, e.g., ML, ML_2, and ML_3. The first description of this stepwise complex formation was published by Bjerrum [13] and its mathematical model can be adapted by characterizing the acid-base properties of multivalent acids and bases.

However, equilibria (and labile systems) are observable "everywhere," such as in solvents (e.g., autoprotolysis of water and ammonia) as well as in organic (e.g., ester formation) and inorganic compounds (e.g., mixtures of boron-halides [12b] and Fe(III)-Fe(II) redox equilibria) in biochemistry (Michaelis–Menten kinetics).

Complicated labile systems are described by their composition matrix [14a], where each component belongs to one column and each row represents one species with a unique composition. The elements of the matrix are stoichiometric numbers and each species should be described by its formation (overall/cumulative stability) constant (log β). Table 1 shows two representative component matrices. Binary, ternary, or quaternary systems are considered if the number of components is 2, 3, or 4, respectively.

Table 1

Two representative component matrices: **a**: the binary system of H^+–GlyGly and **b**: the ternary system of H^+–GlyGly – Cu(II); data taken from Ref. [15] (I = 0.2 M KCl, t = 25°C)

a	H^+	GlyGly	log β	**b**	H^+	GlyGly	Cu(II)	log β
LH	1	1	8.13	CuL	0	1	1	5.56
LH_2	2	1	11.30	$CuLH_{-1}$	–1	1	1	1.33
				$CuLH_{-2}$	–2	1	1	–8.04
				CuL_2H_{-1}	–1	2	1	4.46

These matrices can be used to predict the individual concentrations (the speciation) of all the species formed in any set of component concentrations (see Section 3.1). As the determination of speciation is equal in practice to the determination of the composition matrix with the formation constants, and many individual species distribution (a "speciation") can be calculated from this matrix, then the word "speciation" sometimes has a second meaning, which is the composition matrix itself (including the formation constants).

Labile systems are first studied in fixed conditions (constant T, p, or I), starting from the simplest binary systems and possibly without any matrix effect, by using non-invasive (which does not alter the equilibrium state) methods such as potentiometry or spectroscopy. The concentrations of the species measured under different conditions or component concentrations can be used to determine the formation constants (log β). If sufficient data are obtained, they can be used to perform modeling calculations in order to describe real/complex

systems in any experimental conditions. The result of these calculations may be confirmed by structural investigation methods.

2.2. Inert systems

In practical completely inert systems, there is no component exchange between the species, with no association and dissociation processes, and thus the species are separable from each other. For example in a mixture of H_2-D_2 in ambient conditions, there are no species such as DH and their physical separation is possible. By contrast, DHO also appears in the labile D_2O-H_2O system and the separation of various species is much more complicated. For complexes of certain 3d metal ions, such as Cr(III) (d^3) and Co(III) (d^6), the ligand exchange reactions are very slow, which were studied extensively by Werner [16]. The crystal and ligand field theory [17] can explain the lability and inertness of different transition metal ions.

In inert systems, there is (usually) no suitable data set for use in speciation prediction or modeling calculations, so further analyses in other experimental conditions are required to determine sufficient information about all the species that can be formed. In these systems, speciation refers to the concentrations determined or the concentration ratios of the species identified. In order to determine the concentration matrix in "real" samples, any type of analytical method can also be used, even a destructive one. The most frequently applied method is chromatography [18]. It should also be mentioned that there is no connection between lability, which is a kinetic term, and thermodynamic stability [19].

Many real-world systems lie somewhere between complete lability and inertness. This simply means that it takes more time to reach complete equilibrium, e.g., the HVO_4^{2-}-H^+ system is considered labile at pH > 7, whereas decavanadates are formed at pH < 7, which decompose quite slowly. This system could take more than a day to reach a true equilibrium.

In addition, it is impossible to predict the As(III)/As(V) ratio in a simple way based merely on the As content, but if we know the total concentration of inorganic As(V), the speciation of As(V) (forms such as H_3AsO_4, $H_2AsO_4^-$, $HAsO_4^{2-}$, or AsO_4^{3-}) can be calculated at a given pH using the formation constants of the species at the different protonation states.

3. Development of the application of speciation in chemistry

3.1. Species distribution calculations from equilibrium constants

Species distribution curves represent the percentages (or partial mole fractions) or equilibrium concentrations of the different chemical species present in a solution under given conditions in a representative manner [20]. Concentration distribution curves are generally presented as a function of a single variable, such as pH, where the fixed values of the components (reagents) uniquely determine the molar ratios of the species formed.

The equilibrium concentrations of various species are computed by solving the system of mass balance equations constructed for each component (Eqs. 1–3 for a system containing three components: M, L, and H), and these mass balance equations are then solved iteratively for the concentrations of the free components. In addition, it is necessary to know the stoichiometry and overall/cumulative stability constants ($\beta(M_pL_qH_r)$) of all the associations (e.g., ligand species, LH_r; metal complexes, $M_pL_qH_r$; and metal hydrolysis products, M_pH_r; where p, q, and r are the stoichiometric numbers of the components in the given species) and the ionization constant of water (K_w). $\beta(M_pL_qH_r)$ is defined for the general equilibrium shown in Eq. 4, where M denotes the metal ion and L is the completely deprotonated ligand.

$$c_M = [M] + \sum_{i=1}^{n} p_i \beta_{pqr} [M]^{p_i} [L]^{q_i} [H]^{r_i} \quad (1)$$

$$c_L = [L] + \sum_{i=1}^{n} q_i \beta_{pqr} [M]^{p_i} [L]^{q_i} [H]^{r_i} \quad (2)$$

$$c_H = [H] + \sum_{i=1}^{n} r_i \beta_{pqr} [M]^{p_i} [L]^{q_i} [H]^{r_i} \quad (3)$$

$$pM + qL + rH \rightleftharpoons M_pL_qH_r \text{ as } \beta(M_pL_qH_r) = [M_pL_qH_r]/[M]^p[L]^q[H]^r \quad (4)$$

Various computer programs have been developed to produce distribution diagrams for the species formed in solution, such as HYSS [21], Medusa [22], PSEQUAD [23], DISDI [24], and BEST [25]. The speciation distribution curves calculated for compounds containing dissociable protons represent the fractional contribution of each protonated (LH_r) and unprotonated (L) species in equilibrium, and thus the average number of protons bound and the actual charge of the ligand can be viewed as a function of the pH. As a simple example, a single metal-one ligand system species distribution diagram was calculated for the Cu(II) complexes formed with GlyGly at a metal-to-ligand ratio of 1:2 and at millimolar concentrations based on previously reported data [15], as shown in Fig. 1a. The diagram

clearly shows that the complexation process starts with the formation of the mono-complex $[Cu(GlyGly)]^{+}$ at pH > 3.2, prior to the deprotonation of amide group, and the complex $[Cu(GlyGly)H_{-1}]^{0}$ predominates in the neutral pH range. The bis-ligandum complex $[Cu(GlyGly)_2H_{-1}]^{-}$ and ternary hydroxido-species ($[Cu(GlyGly)_2H_{-2}]^{2-}$) also form in the basic pH range. In order to represent the effect of the metal-to-ligand ratio on the fate of the $[CuGlyGlyH_{-1}]^{0}$ complex in solution, speciation curves were computed as a function of the total concentration of GlyGly at pH 7.4, as shown in Fig. 1b, which indicates that a quite high ligand excess (tenfold) is necessary for the complete formation of $[Cu(GlyGly)_2H_{-2}]^{2-}$.

Speciation curves can be computed for ternary (mixed metal or mixed ligand) or multicomponent systems with increasing numbers of components. Predominance curves calculated for a hypothetical M–L^1–L^2–H system, where the formation of only binary $M_pL^1{}_q$ and $M_pL^2{}_q$ complexes is assumed and the ligands are in equimolar amounts, are advantageous for comparing the relative metal ion-binding abilities of ligands in the selected pH range [26]. This approach is especially useful when the cumulative stability constants are not directly comparable. However, as the numbers of components and associations increase, the situation becomes closer to more complex real-world samples such as biofluids (e.g., human blood serum) and natural aquatic systems (e.g., surface or ground water). Blood serum contains 20 essential amino acids (AA), 12 essential metal ions, more than 100 LMM ligands, and numerous HMM components (such as proteins) with potential metal ion-binding abilities [27-29]. To determine the serum (or plasma) speciation of a particular metal ion or metal complex, it is necessary to define a series of chemical equilibria that represent the system, where knowledge is necessary of the stoichiometry and cumulative stability constants of all associations, including the binary and ternary complexes formed with the LMM and HMM serum compounds, and the total concentration of the components. Several speciation modeling calculations for the distribution of metal ions or metal complexes in human blood serum have been discussed in previous reviews [27-30]. The computer program ECCLES [31] can be used to predict the speciation of metal ions/complexes (or ligands) in biological fluids (see Section 4), although it can only operate with LMM ligands by assuming that the HMM components have a weaker impact in controlling the distribution of metal ions due to the generally slow interaction kinetics of proteins. However, protein–metal equilibria cannot be excluded, especially in faster complexation processes with the proteins. Indeed, protein interactions were included in computer simulations of the distributions of Al(III) [32], V(IV)O [33], Zn(II) [34], Ga(III) [35], and Gd(III) [36] complexes in serum. In the case of

speciation in natural/industrial waters, the redox processes, solubility properties, and adsorption interactions must also be considered (see Section 4.2).

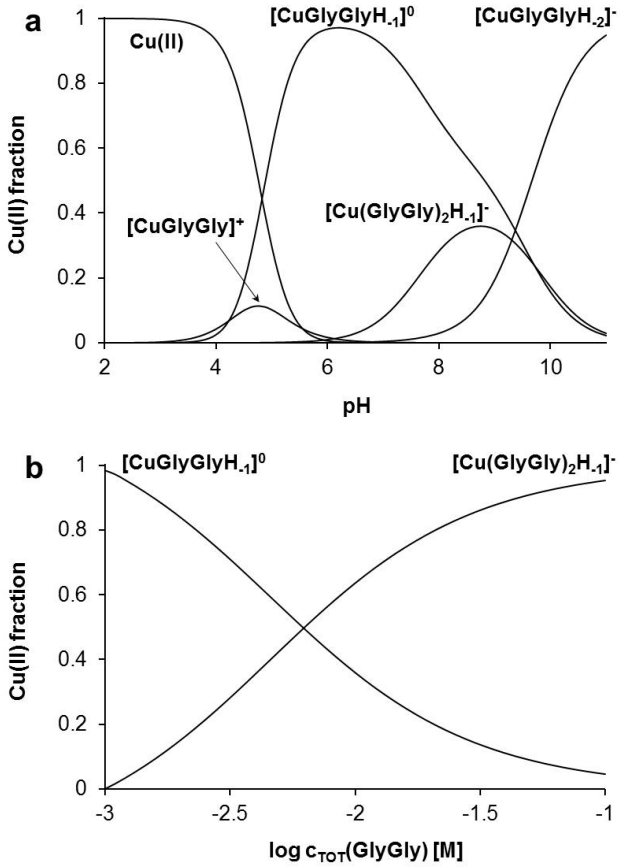

Fig. 1 Concentration distribution curves for the Cu(II) – GlyGly system: (a) between pH 2 and 11 ($c_{Cu(II)}$ = 1 mM, c_{GlyGly} = 2 mM), and (b) between c_{GlyGly} = 1 mM and 10 mM ($c_{Cu(II)}$ = 1 mM, pH = 7.4). Calculations were performed using the protonation constants of GlyGly and the overall stability constants of the Cu(II) complexes (I = 0.2 M KCl, t = 25°C) taken from Ref. [15].

A large number of significant metal–ligand stability constants and associated thermodynamic data have been critically evaluated by IUPAC and selected values have been recommended. The SC-Database provides access to published stability constants for metal complexes of *ca.* 9800 ligands [37], although data for HMM compounds are limited.

It should be noted that the thermodynamic equilibrium constants are based on activities that depend on temperature and pressure. Most reported stability constants are considered as stoichiometric constants, which are expressed as equilibrium concentration quotients, and thus they are valid only at a given ionic strength (I) and in a given medium. The activity is

proportional to concentration, where the proportionality constant is the activity coefficient (γ) that brings the stoichiometric constant close to the thermodynamic constant. This is why the ionic strength must be kept constant during experimental determinations of stability constants. The mean activity coefficient ($\gamma_{\pm}$) of a dissolved electrolyte depends on the ionic strength and it can be calculated in diluted solutions according to the Debye–Hückel theory [38], or in high ionic strength solutions using the Pitzer interaction model [39]. The thermodynamic constants are referred to zero ionic strength, so they can be calculated when the activity coefficients are known, or obtained by extrapolating the stoichiometric constants determined at various ionic strengths according to the Davies equation [40]. The conditional stability constants introduced by Schwarzenbach [41] also consider other equilibria that occur simultaneously with metal–ligand complex formation such as (de)protonation processes of the ligand and the hydrolysis of metal ions. Thus, conditional stability constants are valid only under the given pH value and conditions.

Selecting adequate equilibrium processes and applying reliable stability constants are essential for calculating speciation curves. The most problematic issue that affects rigorous mathematical modeling calculations of the distribution in a multicomponent systems is the lack of suitable stability constants that are relevant to the given conditions (e.g., in the case of the human serum: t = 37°C, I = 0.10 M NaCl, pH = 7.4). More thermodynamic data are increasingly being published and the calculations can be run easily due to advances in computer software, but the predicted distributions and transformation processes for metal ions or complexes often have limitations. Therefore, computational modeling still cannot replace controlled instrumental methods for determining speciation, although it provides a very important alternative approach and it can be helpful understanding experimentally obtained findings and reduce the experimental effort required.

3.2. Parallel application of speciation and solution structural investigations

Structural investigations of solutions mainly based on spectroscopic measurements can be used to confirm speciation/equilibrium data. These methods are usually required because of the limitations of pH-potentiometry and other thermodynamic methods. However, these methods measure non-selective effects, e.g., proton liberation, which are insufficiently sensitive to detect minor processes/species. Thus, in order to use any spectroscopic method in quantitative data evaluations, the concentrations of the individual species formed should be calculated from the information obtained.

For example, pH-potentiometry cannot be used above or below a certain pH value, at a low L/M ratio, or when the measureable concentration or pH range is reduced, e.g., because of the low solubility of a complex. Furthermore, some complex formation reactions might not be pH-sensitive, such as oligomerization processes, which cannot be detected directly by pH-potentiometry. Excessively high or low stability constants are also problematic because the formation equilibrium for these species can only be partially observed or not at all in the measurable pH range, so the stability constants cannot be determined with sufficient accuracy by pH-potentiometry [14b]. Similar problems may also occur during the evaluation of calorimetric, kinetic, or cyclic voltammetric measurements.

In order to perform joint evaluations of pH and spectral data, the experimental conditions should be kept the strictly same, as required with pH-potentiometry (i.e., constant I, T, and pH calibration method). The data obtained from different spectroscopic measurements can also be combined. Spectroscopic approaches are sometimes used only to determine conditional stability constants, such as measurements at a certain pH.

The advantages of spectroscopic methods may include the more accurate detection of minor species and the more appropriate determination of the number of the species formed. Even if the spectral bands overlap with each other, such as in UV-visible (UV-Vis) spectrophotometry, matrix rank analysis of the whole data set can yield appropriate values for a number of colored species [42]. The practical disadvantages of spectroscopic methods compared with pH-potentiometry include the lower number of data points collected and less accurate measurements of the necessary pH values.

The speciation determined by spectroscopic methods may be referred to as structural speciation, which does not always agree with the thermodynamic speciation. A metal complex with a given composition may have more than one structure (isomers such as fac-mer isomerism) [43]. In addition, changes in composition do not always lead to changes in the spectra. For example, the protonation of a ligand at a non-coordinated moiety located far from the coordination sites will not change the observed d-d bands or the electron paramagnetic resonance (EPR) spectra of a 3d metal ion [44]. The equilibria of the structural speciation (appearance of isomers) sometimes can be described perfectly by microconstants [45,46] (together with the formation constants), but an incompletely verifiable assumption is needed in most cases, which makes the results questionable. In the following sections, examples based on the application of UV-Vis, circular dichroism (CD), nuclear magnetic resonance (NMR), and EPR spectroscopy, as well as fluorimetry and mass spectrometry (MS), are

discussed for obtaining speciation information. More detailed discussions of the spectroscopic methods can be found in other papers in this special issue.

3.2.1. UV-Vis, circular dichroism, and fluorescence spectroscopy

If the absorbance follows the Lambert-Beer law, UV-Vis spectroscopy can be used to determine the concentration of each individual species and the data set obtained can be jointly evaluated with pH-potentiometric data. However, the data include an extra parameter set comprising the molar absorbances (spectra) of all individual species formed. The UV bands usually overlap with each other, so it is sometimes impossible to correctly determine the molar absorbances of the minor species, where the errors increase with the number of species with unknown molar absorbances. CD spectroscopy can be used in a similar manner to UV-Vis spectroscopy in speciation studies, but only optically active species can be detected.

Transition metal complex formation can be monitored based on either the d-d bands (higher concentrations used), the ligand to metal transfer bands, or the metal to ligand charge transfer bands (lower concentration used). The d-d bands are forbidden transitions that result in low molar absorbance values, so they are often not sufficiently sensitive to measure complex formation at millimolar or lower concentrations. The charge transfer and ligand bands are usually more intense, and the optimal concentration is around 100 times lower.

The requirement for a CD signal is that an asymmetric center should be near the chromophore [47]. The advantage of this method compared with UV-Vis spectroscopy is that not each complex formed is CD-active and this technique usually provides more resolved sets for both the d-d and CT transition bands than the simple UV-Vis absorption spectra. For example, complexes of tri- and dipeptides have been studied extensively using CD spectroscopy [48,49]. The correlations between the configuration of the complex and the sign and intensity of the CD bands observed in the CD spectra can be understood or interpreted using the double octant or hexadecant sector rule [50].

Fluorimetry is only applicable to fluorophore ligands and at quite low concentrations, where this method is frequently used to determine the pK_a values of fluorophore components (e.g., see Ref. [51]). The advantage of the method is its selectivity and applicability at more biologically relevant low concentrations (c ~10^{-5} to 10^{-7} M). It should be noted that the proton dissociation constant of a ligand may differ in the excited and ground state in certain cases, which may hinder the determination of the ground state pK_a value. In metal complexes, the effect of dilution on actual speciation is also an important issue because the dissociation of a

complex is more pronounced at lower concentrations than higher concentrations by several orders of magnitude. However, high sensitivity may also be a disadvantage because any type of impurity, even from the solvent, can disturb the equilibrium at a low concentration. It is quite unusual to use fluorimetry in metal-ligand systems because all the non-fluorescent species can absorb the excitation or emitted light. Furthermore, all fluorimeters measure the intensity signal in arbitrary units, and thus the spectra measured with different fluorimeters are not directly comparable. However, if the bound and unbound ligand have fairly distinct fluorescent properties (such as fluorogenic ligands), and the metal complex(es) formed have relatively high solution stability, then fluorimetry is an efficient tool for determining formation constants, e.g., for Ga(III)–8-quinolinol complexes [43].

3.2.2. Nuclear magnetic resonance spectroscopy

Many metal ions are paramagnetic, which leads to shorter relaxation times, a wide chemical shift range, and broadened NMR signals. Thus, complex formation by some of the most frequently studied metal ions (e.g., Fe(II)/(III) and Cu(II)) cannot be studied easily by NMR spectroscopy [52].

In diamagnetic samples, the equilibrium can have two different profiles.

(1) If fast exchange processes occur, the NMR spectrum has a single signal, which is averaged according to the proportions of the partial mole fractions for the active nuclei found in various chemical environments [14c,53]. If the conditions vary, such as the pH or ligand-to-metal ratio, then the partial mole fractions and the chemical shift will change. The simplest example of this behavior is the protonation equilibrium of an organic ligand, where the chemical shift(s) include information about the equilibrium, and the protonation constants of a ligand can be calculated based on the pH-dependence of the observed chemical shifts [54]. The effect of averaging is also apparent in the reciprocal relaxation times and these data may be used to study equilibria where paramagnetic species also participate.

(2) If slow exchange processes occur, all of the various chemical environments are represented by separated signals in the NMR spectra. The integrated intensities of the bands are proportional to the (equilibrium) concentrations of the species. The number of complexes formed and the stability constants can then be determined easily [14c]. The peak areas include information about the equilibrium (it should be noted that a correct pulse sequence is needed for NMR measurements if the data are to be used in qualitative evaluations).

If the exchange rate frequency (Hz) of the chemical environments is comparable to the difference in the chemical shift of the individual signals, then case 1 or case 2 cannot be clearly observed.

The most frequently used ^{1}H- or ^{13}C-NMR spectroscopic methods can be employed to follow simple protonation processes in organic ligands (the labile protons are usually not observable in protic solvents such as water, although peptide protons are generally visible at pH < 5) as well as for studying complex formation with metal ions. The exchange rate of complex formation depends greatly on the type of metal ion, e.g., only fast equilibria are usually observable for Zn(II) upon complexation [55], whereas all the species formed can be detected separately if the ligand exchange is sufficiently slow, e.g., Pd(II) complexes [56]. However, slow and fast exchanges can appear in the same system, as well as in the same spectrum, and in the same species (Fig. 2). In the Ru(II)(η^6-$_p$-cymene)]–thioallomaltol system, the ligand exchange rate is high between the free ligand and the ligand bound in a monodentate (S) manner, but slow between the ligand bound in a monodentate (S) or bidentate (O^-,S) manner [57].

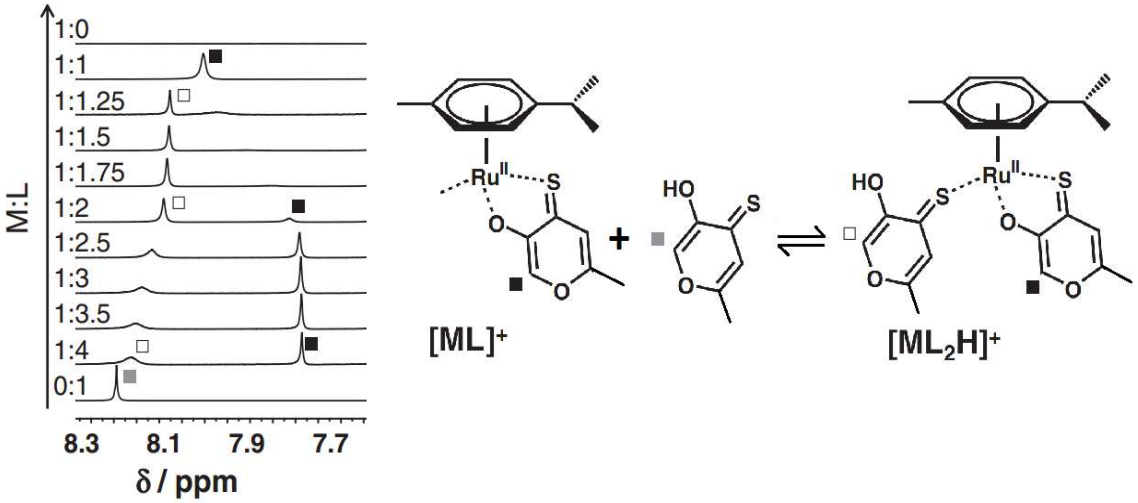

Fig. 2 Part of the low-field regions of ^{1}H NMR spectra recorded for the [Ru(II)(η^6-p-cymene)]–thioallomaltol system at the metal-to-ligand ratios indicated. C*H*(6) protons of the ligand: unbound ligand (■), ligand bound via (O^-,S) (■), and ligand bound via (S) (□). Adapted from Ref. [57].

Similarly, the presence of slow and fast exchanges can be observed in many cases in the ^{51}V-NMR spectra of the H^+-HVO_4^{2-} system [58,59].

Table 2

Periodic table of elements for which the speciation/equilibria were determined based on specific nuclei. The numbers represent previous studies that mentioned the NMR-detectable nuclei for the given element. Upper number: studies related to speciation; lower number: studies related to stability constants/equilibrium constants and/or speciation. The search was performed using SciFinder [60].

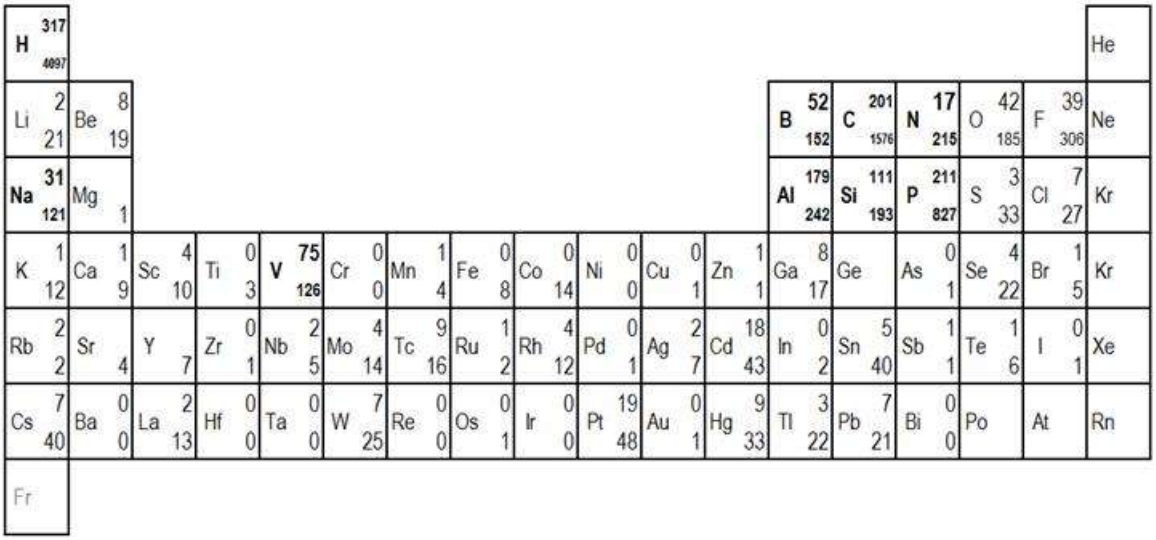

It would be interesting to identify the NMR measurements of nuclei that are used frequently to determine speciation or equilibrium/stability constants (see Table 2). Indeed, it seems that three different parameters determine these numbers: (1) the commonness of the application, (2) the technical difficulties of obtaining NMR measurements for certain nuclei, and (3) the overall importance of the element in speciation chemistry. Based on Table 2, the metal-ligand equilibria are monitored more frequently based on one of the nuclei of the ligand rather than that of the metal ion. The most frequently used nuclei are the classic (^{1}H, ^{13}C) organic nuclei, but others (^{15}N, ^{17}O, ^{31}P, and ^{19}F) are also often used to monitor the chemical environment of the ligand. The importance and commonness of C, N, and O exceed the technical difficulties involved in their determination (low abundance and receptivity). The importance is similar for P and S, but because it is easy to measure and interpret the ^{31}P-NMR spectra, these are much more common, and the same is true for ^{19}F.

The most frequently studied metal nuclei are ^{23}Na, ^{27}Al, ^{29}Si, and ^{51}V, but ^{195}Pt, ^{119}Sn, ^{113}Cd, ^{183}W, ^{199}Hg, and ^{205}Tl are also measured often. If the number of protons in the nuclei is an odd number, the natural abundance of the NMR active nuclei is usually much higher than that with an even number. It would be interesting to study Ca/Mg as well as Na, but the large difference in the natural abundance of the NMR active nuclei leads to their significantly lower

usage. It is easy to measure ^{27}Al and ^{51}V (only in the oxidation state of V) but their overall importance is less significant than that of Fe/Cu, or even Pt/Hg. It should also be mentioned that the paramagnetism of transition metal ions also hinders their measurement.

3.2.3. Electron paramagnetic resonance spectroscopy

EPR spectroscopy is a powerful ion-specific method in some cases. As mentioned earlier, most of the common 3d transition metal ions are paramagnetic and they are targets for EPR investigations, although the spectra or spectral changes are not always sufficiently informative to perform speciation studies based on EPR alone. The most frequently studied ions are Cu(II), V(IV)O, Fe(III), and Mn(II) (see Table 3). Cu(II) has been studied most frequently due to the same reason given for NMR, i.e., it is easy to measure, the spectra are informative, and the overall importance of Cu(II) is high. The detectability of V(IV)O is similar to that of Cu(II), but it is much less important. Fe(III) is also important but its spectra are less informative in a similar manner to Co(II). There are also unresolved issues, e.g., Nb(IV) has easily detectable informative spectra but the 4+ oxidation state is not as common for Nb as 5+, and its equilibria are also of less interest. Due to the higher inertness of the 4d/5d transition metal ions and their complexes, there is no reason to study their speciation by spectroscopy.

Systems that contain odd numbers of electrons (d^1: V(IV)O, d^3: Cr(III), d^5: Mn(II)/Fe(III), d^7: Co(II), d^9: Cu(II)) can usually be measured at room temperature with the most common X-band EPR instruments. Measuring the EPR spectra of ions with an even number of electrons usually requires a lower temperature and/or higher frequency, so equilibrium studies of these systems are rare.

Table 3

Transition metal components of the periodic table of elements for which the speciation/equilibria of the ions were determined by EPR. The numbers represent studies that mentioned the element: upper numbers = studies related to speciation, lower numbers = studies related to stability constants/equilibrium constants and/or speciation. The search was performed using Scifinder [60].

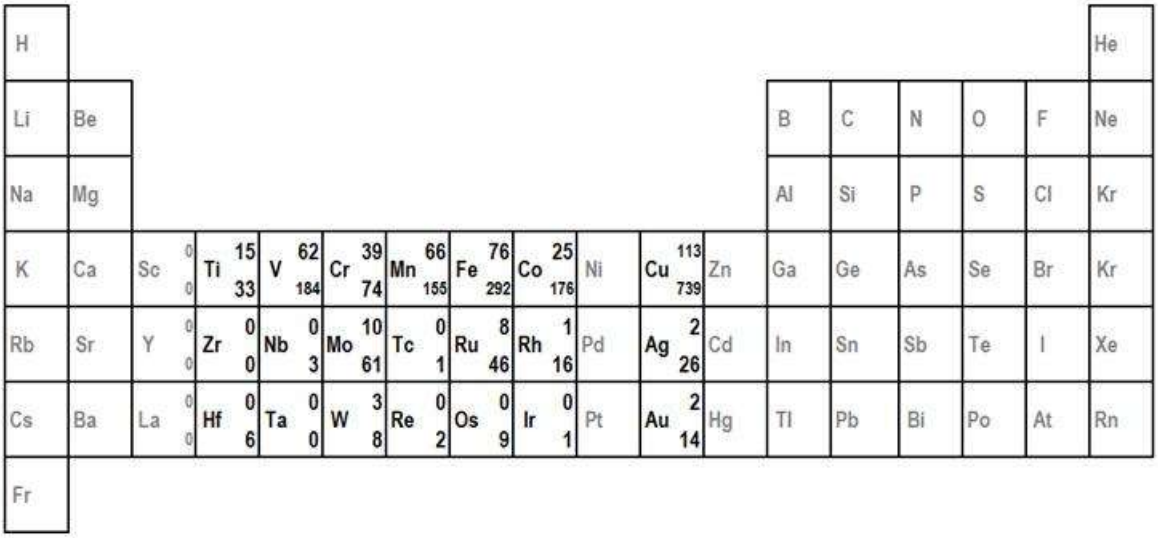

Based on the EPR spectral parameters (g, A) of Cu(II) and VO(IV) complexes ([61, 62]), assumptions can be made regarding the nature of the coordinating donor atoms. The anisotropic spectra measured at liquid nitrogen temperature are usually more informative for solution structural predictions, but the molar ratios derived from these spectra are not always directly comparable with other speciation results measured at room temperature due to the shift in temperature.

The advantage of EPR spectroscopy compared with other techniques (e.g., UV-Vis and CD) is that the measured spectra (room temperature, isotropic) can be simulated perfectly using only a few parameters (g_0, A_0, and bandwidths; e.g., α, β, and χ values for Cu(II)). This makes the determination of the number of species formed and their identification more appropriate and accurate.

A unique application (2D EPR) [63] can handle mathematical equilibrium data (formation constants and log β), conditional data (total concentrations of the components and pH), and EPR parameter sets (e.g., g_0 and A_0 for all species) to simulate all the spectra measured at various pH values and different metal-to-ligand ratios.

3.2.4. Mass spectrometry

This very rapidly developing area of analytical chemistry has also influenced speciation studies, where it can be used to identify the compositions of the species formed in solution [64]. This method is appropriate for application to inert systems, but it is destructive and can disrupt any equilibrium or speciation in labile systems. Therefore, it is quite difficult to interpret the data if the mass spectra disagree with the findings obtained using other methods.

The electrospray ionization-mass spectrometry (ESI-MS) method is used widely to identify metal complexes present in solution [65], although the spectra can only be trusted for qualitative rather than quantitative purposes.

3.3. Modeling calculations in biological or environmental systems using stability constants and their experimental confirmation

In real-world systems, numerous species can be present in different proportions, e.g., the majority of the metal ions are bound to proteins in biological fluids and only a small proportion is bound to LMM compounds, such as AAs, biophosphates, carboxylates, and hydroxycarboxylates. Free transition metal aqua ions only exist in extremely low concentrations in biological fluids, so they cannot play significant roles in biological processes. By contrast, metal ions bound to LMM compounds have key roles in many biological processes, such as intestinal and cellular absorption, transport processes, and excretion. These are the mobile forms of metal ions. Understanding these processes requires accurate knowledge of the equilibria that determine the relative proportions of the LMM and protein-bound fractions. Specific experimental techniques are available to separate and determine LMM and HMM bound metal ions. Fractionation is a very important aspect of the speciation of trace elements, which usually involves coupling an analytical separation technique directly to a metal-sensitive detection system. Detailed discussions of chemical speciation in various biological fluids and tissues as well as examples of the application of various methods for determining the distribution of trace elements in biological systems are provided in the “Handbook of Metal Ligand Interactions in Biological Fluids” edited by Berthon [66], and in “Chemical Speciation in the Environment” edited by Ure and Davidson [67]. However, it is difficult to apply any structure elucidation techniques to explore the complete speciation of a metal ion due to the small quantities (usually micrograms) of the analyte. By contrast, computer programs developed to deal with multiple chemical equilibria can be employed to calculate speciation for laboratory solutions, as well as for conducting simulations of naturally occurring mixtures of metal ions and ligands in biological and environmental samples.

These programs are employed increasingly frequently to determine chemical speciation in very complex systems and ECCLES is one of the most widely used simulation programs [31]. Computer programs require a rich and reliable database of stability data for all the

metal-ligand interactions that may occur in biological fluids. The most complete database available, which is for blood plasma, includes a set of about 10,000 complexes of ca. 10 essential and toxic metal ions, over 1,000 ligands, and the results for different plasma conditions. As an illustration, Table 4 shows the distribution of Cu(II) in plasma according to the LMM constituents calculated using the ECCLES program.

Table 4

Calculated distribution of Cu(II) bound to LMM constituents of human blood plasma (based on data in Ref. [31]).

Cu(II)	%	Cu(II)	%
Cu(His)(Gln)	19	Cu(His)(LysH)$^+$	4
Cu(His)$_2$	16	Cu(His)(Gly)	4
Cu(His)(Thr)	15	Cu(His)(Asn)	4
Cu(His)(Ser)	8	Cu(His)(Val)	4
Cu(His)(Ala)	5	Cu(His)(Leu)	4

The weakness of this model calculation approach is the lack of the necessary data. Therefore, the stability constants of binary and ternary metal ligand systems need to be determined in advance by focusing on the most important and strongest binders, and thus a good estimate can be obtained easily and simply. This approach was employed to obtain simulations of the serum distribution of various insulin-enhancing V(IV) [33,68,69] and Zn(II) complexes (see Section 4.3.1) [70]. In the ideal case, the calculated results can be confirmed by separation methods or structure elucidation techniques [70].

The experimental confirmation of modeling calculations is important for insulin-enhancing metal compounds. Detailed speciation and spectroscopic methods have shown that under biological conditions, in the case of the V(IV)O containing antidiabetic compounds human serum transferrin (Tf) is the main V(IV)O transporter in the serum [33,68,69], whereas human serum albumin (HSA) is the main transporters in the case of the Zn(II) complexes [34]. Modeling calculations can determine the detailed distributions of metal ions among the LMM and HMM components of serum. Various separation techniques such as ultrafiltration [70] and capillary zone electrophoresis inductively coupled plasma MS (CZE-ICP-MS) [34] have been employed in the fractionation of different LMM and HMM fractions to confirm the basic findings of the modeling calculations, e.g., the distribution of Zn(II)–dipic complexes in serum systems (0.1 mM, serum diluted with buffer: 1:4, 24 h incubation at 25°C), where most

of the Zn(II) was bound to HSA, although a minor amount of Zn(II) was bound to dipic, whereas no Zn(II) was bound to Tf (Fig. 3).

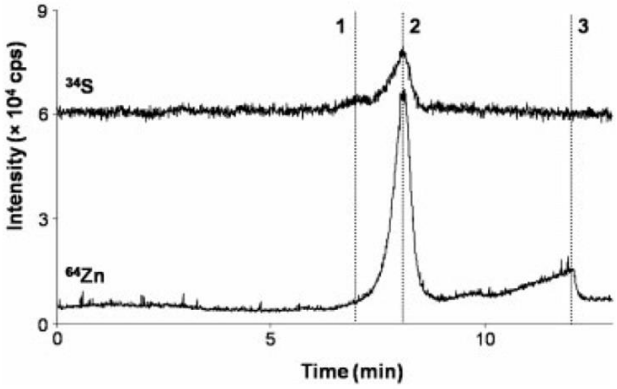

Fig. 3 Electropherogram of $[Zn(dipic)_2]^{2-}$ after incubation for 24 h with blood serum diluted 1:4 with incubation carbonate buffer. Traces are shown for ^{64}Zn and ^{34}S (for HSA and Tf detection). Peak identification: 1 = Tf; 2 = HSA adduct and 3 = $[Zn(dipic)_2]^{2-}$.(dipic: 2,6-dipicolinic acid, c($[Zn(ligand)_2]$) = 100 μM, pH = 7.40; T = 25°C). Adapted from Ref. [34]

Environmental samples can be just as complicated as biological samples. Mercury is usually present in natural waters at trace or ultra-trace levels, which presents a formidable challenge to even the most up-to-date sampling, sample handling, and analytical procedures for determining mercury in environmental samples.

The major inorganic and methyl mercury species in seawater and fresh water environments have interesting distributions. Calculations predict that divalent mercury, Hg(II), should exist predominantly as chlorido complexes in sea water, but the major chemical forms of mercury in fresh water systems are chlorido, hydroxido, and mixed species. The relative proportions of the latter species depend greatly upon the pH of the medium. However, the validity of computational methods for determining the speciation of mercury needs to be tested based on reliable data obtained using one or more experimental methods [71].

Current methods only allow the classification of several common mercury species into operationally defined categories according to specific physical or chemical properties. A suitable analytical method (Fig. 4) is a variation of the classification scheme described by Lindqvist and Rodhe [72], where parts of this procedure have been applied to analyze mercury in environmental samples. However, very few published results have been obtained using the entire scheme. The initial separation into particulate and dissolved forms of mercury

is usually affected by filtration (filter medium with a pore size of 0.45 μm). Volatile species such as elemental mercury and dimethyl mercury can be readily separated from nonvolatile forms (e.g., $HgCl_2$, $Hg(OH)_2$, and CH_3HgCl) by gas stripping ("purge and trap") techniques. Differentiating "reactive" and "non-reactive" species is usually accomplished in one of two ways: either "reactive" forms are reduced to elemental mercury by stannous chloride (in acid solution) or "non-reactive" compounds are reduced (to Hg(0)) by $NaBH_4$; or "nonreactive" forms are converted into "reactive" forms by treatment with concentrated HNO_3. In this scheme, mercuric halides, HgX_2, mercuric hydroxide, $Hg(OH)_2$, and Hg(II) complexes with organic acids are treated as "reactive" forms, whereas the "non-reactive" forms include monomethyl mercury species, CH_3HgX, mercuric sulfide, HgS, and sulfur-containing organomercury complexes [71]. The results obtained by this experimental separation of various mercury species can be compared with the results of fractionation calculations.

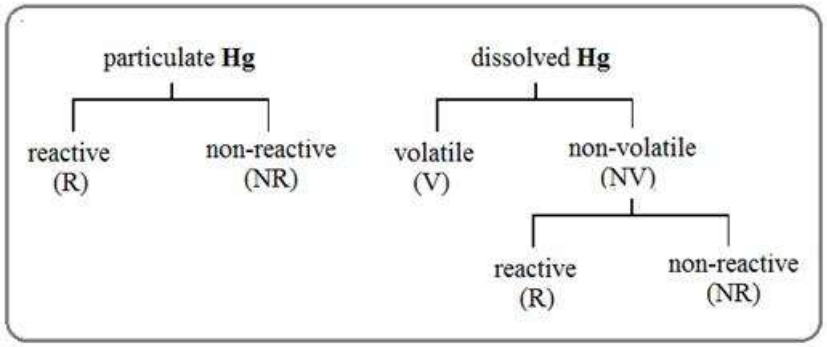

Fig. 4 Classification scheme for Hg species in natural waters. (Based on Ref. [66].)

4. Examples of the applications of speciation: analysis and modeling calculations

4.1. Chemical speciation in trace analytical and environmental chemistry

Previously, most trace analytical measurements focused on the total amount of a specific element (such as toxic elements, including arsenic, mercury, or cadmium, and elements that are necessary for living organisms, including selenium and magnesium), because most atomic analysis techniques are destructive. At present, it is generally accepted that the biological availability, toxicity, cellular uptake, and trafficking of metal ions/metal

complexes depend greatly on their actual chemical and physical forms, oxidation state, etc., and not merely on their concentrations [73]. For example, the LD_{50} values (rat) of inorganic arsenic species are between 3–20 mg/kg, but higher than 10000 mg/kg for organic compounds such as arsenobetaine [74]. Chemical speciation studies must be performed to obtain more reliable information about any sample. In order to determine the specific forms/species of an element, they must first be separated before reaching a destructive detector [73]. In general, the appearance of multiple forms is described by speciation, whereas the process employed for obtaining quantitative estimates of the contents of different species is called speciation analysis [74].

The levels of speciation considered by trace analytical chemistry are as follows [74].

i) Screening speciation: Search and determination of selected chemical species.

ii) Group speciation: Search and determination of groups or classes of selected species.

iii) Distribution speciation: Search and determination of selected chemical individual types of particular elements in analyzed samples.

iv) Individual speciation: Search and determination of all chemical individual types present in a sample.

Table 5

Application areas for speciation trace analysis [74]

Element		**Application area for speciation analysis**
Aluminum	Al	Aggregates [75]
Antimony	Sb	Redox forms and organoantimony compounds in the environment [76,77]
Arsenic	As	Redox forms and organoarsenic compounds in the environment [77] Arsenic in food products [78] Forms of arsine in air [79]
Cadmium	Cd	Cadmium in food products [80]
Chromium	Cr	Redox forms of chromium, Cr(VI) in the environment [81,82]
Lead	Pb	Forms of lead compounds in the environment [83]
Mercury	Hg	Forms of mercury compounds in the environment [84-86]
Selenium	Se	Inorganic and organometallic selenium compounds in the environment [87]
Thallium	Tl	Thallium compounds in river water [88]

Tellurium	Te	Tellurium compounds in the environment [89]
Uranium	U	Forms of uranium compounds in seawater [90]
Zinc	Zn	Forms of zinc compounds in the environment and food [91]

The usual analytical procedure comprises filtration (to obtain the soluble and insoluble fractions), separation from the matrix and fractionation (e.g., by high-performance liquid chromatography (HPLC), size exclusion chromatography (SEC), gel permeation chromatography, anion/cation exchange chromatography, CZE, ultrafiltration, dialysis or gas chromatography in the case of volatile species). The isolated species are then determined by atomic absorption spectrometry, flame atomic absorption spectrometry, ICP-optical emission spectrometry, ICP-MS, MS, fluorimetry, atomic fluorescence spectrometry, UV-Vis, or electrochemical methods depending on the type of analyte [74].

Chemical speciation is also essential for many environmental problems, but the direct instrumental determination of metal ion/complex distributions in biological and environmental samples has several difficulties: i) the identification and selective determination of different species are challenging due to the lack of adequate reference materials, ii) the technique employed can disturb and shift the chemical equilibria, and iii) few methods are appropriate for the detection of species present at ultra-trace levels. In addition, speciation analysis is fairly difficult in complex matrices such as sediments, soils, aerosols, and fly ash.

Numerous previous reviews [92-98] and book chapters [99-102] have summarized the most important procedures and findings related to speciation determination for different essential and toxic metal ions in a wide variety of environmental samples. The speciation of metallic (and some non-metallic) compounds that cause human health risks was reviewed in detail by the WHO Environmental Health Criteria Program [103]. Assessments of the most significant examples are considered in the present review for elements related to acute toxicity (e.g., Cr, Ni, As, Hg, and Ba), carcinogenicity (e.g., Cr, Ni, and As), lung toxicity (Co), nephrotoxicity (Cd), reproductive toxicity (Ni and Hg), and neurotoxicity (e.g., Mn, Hg, Pb, and Sn) in order to determine the relationship between exposure to environmental pollutants and human health. Reviews have described the speciation of Hg compounds in environmental and biological samples [92,93], Al [94], organolead [95], As [96], Cr in ground water [97], and radionuclides [98].

Due to the complexity of real-world systems and the limitations of analytical methods, speciation determination usually relies on analytical techniques combined with mathematical

modeling calculations. In speciation calculations, sorting the most feasible interactions and associations present in solutions as well as selecting their stability constants from published data can significantly affect the final predicted distribution. Several computer programs have been developed and employed to calculate the concentrations of various chemical species at equilibrium based on a database of equilibrium stability constants for inorganic species encountered in water [104]. In addition to the formation of different metal-ligand complexes, the equilibria between soluble and insoluble phases, as well as the adsorption of colloids must be considered during computational modeling. One problem is that most of the stability data in databases were obtained for metal-ligand species at 25°C [37,105]. However, determining thermodynamic data for the complex formation processes involving the macromolecules or colloids present in natural systems, such as humic and fulvic compounds, polysaccharides and clays, also causes difficulties related to the structural and physicochemical complexity of these complex-forming agents. The most important databases containing experimental results for speciation constants are SC-Database (IUPAC) [37], the National Institute of Standards and Technology standard reference [106], and Joint Expert Speciation System thermodynamic database [107]. The most frequently used programs are JESS [108], MINEQL [109], and MINTEQA2 [110]. These programs contain built-in databases for many chemical equilibria, including complexation, precipitation, dissolution, adsorption and redox reactions. Some also include Debye-Hückel or specific interaction theory parameters for ionic strength correction. Several programs can handle slow reaction kinetics for processes such as adsorption/desorption or precipitation/dissolution.

4.2. Chemical speciation of Al(III) and Fe(III) in water and biology

With the exception of alkaline and some alkaline earth metals, the metal ions in biological systems bind to different LMM or HMM biomolecules during their absorption, transport in biological fluids, and distribution among different organs and excretion processes. The presence of these biomolecules may significantly alter the properties of metal ions in solution. The general solution states of two metal ions, i.e., the essential Fe(III) and toxic Al(III), are considered in pure aqueous solution and biological systems in the following, where their serum transport properties are also presented to explain how the biological milieu affects the solution state/speciation.

4.2.1. Hydrolysis of toxic and essential metal ions: Al(III) and Fe(III)

All equilibrium studies of metal ion-ligand systems in aqueous solution with either essential or toxic metal ions require a speciation model and adequate stability data for the metal ion–OH^- system because the ligand must compete with the OH^- ion for the metal ion to form complexes. This fact has stimulated much research in this field, including the well-known book by Baes and Mesmer [2]. In the following, the results obtained for the hydrolysis of the toxic Al(III) [3] and the essential Fe(III) ion [6] are considered briefly. The speciation of both systems is complex because of the time- and concentration-dependent formation of oligonuclear hydrolytic species.

$[Al(OH)]^{2+}$ is a well-defined species with a pK of ~5.5. At a more acidic pH, only $[Al(H_2O)_6]^{3+}$ exists, whereas only $[Al(OH)_4]^-$ exists in the basic pH range. Between the two extremes, the species present in a slightly acidic to neutral solution are less well defined because soluble polynuclear complexes may also be formed in addition to the solid compound $Al(OH)_3$. This problem is due to the very slow conversion of oligonuclear hydroxido species to larger polynuclear complexes, which are necessary precursors of the macromolecular polymer $Al(OH)_3$. It may take hours or even up to a day to reach thermodynamic equilibrium, which means that soluble hydroxido complexes can be maintained almost indefinitely in a metastable state under conditions where the solid $Al(OH)_3$ is the thermodynamically stable species. The analytical (total) concentration of Al(III) greatly affects speciation [2]. The formation of a highly polymeric species $[Al_{12}(OH)_{32}]^{7+}$ was demonstrated unambiguously in the solid state by X-ray diffraction, as well as in solution by ^{27}Al and ^{17}O NMR [111]. Moreover, the most probable oligomeric species formed in solution are the dimeric $[Al_2(OH)_2]^{4+}$ and trimeric $[Al_3(OH)_4]^{5+}$. An important question concerning the speciation of Al(III) in practical systems is the lowest concentration of Al(III) where the formation of polynuclear species must be considered. Their formation is certainly negligible in biological fluids or tissues, where the concentration of Al(III) can only reach the μM level, but in toxicological studies or environmental samples, various soluble Al(III) species are present in mM concentrations that are not negligible [2].

The hydrolysis of ferric ion-containing solutions is readily induced by dilution or adding a base, where these hydrolytic reactions involve simple deprotonation and more complex oligomerization reactions [112-116]. Initially, at a rather acidic pH, the purple aqua ion $[Fe(H_2O)_6]^{3+}$ liberates one proton ($[Fe(OH)]^{2+}$), which is followed by dimerization ($[Fe_2(OH)_2]^{4+}$) to yield a yellow solution. The equilibria leading to mono- and dinuclear

complexes such as $[Fe(OH)]^{2+}$, $[Fe(OH)_2]^{+}$, and $[Fe_2(OH)_2]^{4+}$ are formed rapidly [117]. The low molecular hydroxido complexes interact to produce species with higher nuclearity (e.g., $[Fe_3(OH)_4]^{5+}$). These polynuclear complexes can be isolated as amorphous species. They comprise iron cores of nuclearity (p) with OH^- and O^{2-} in bridging positions, and they can be represented by the general formula: $Fe_pO_r(OH)_s^{3p-(2r+s)}$. The charged polyelectrolytes can be coagulated under specific conditions or simply by ageing [118]. The coagulation processes can be influenced greatly by various biomolecules, such as proteins, carbohydrates, and lipids, where this process is called biomineralization and it may lead the formation of the ferrihydrite core of ferritin.

4.2.2. Role of human blood serum in transport and distribution processes

Serum is the liquid portion of blood obtained after coagulation, excluding the red and white blood cells, which contains all the plasma proteins such as HSA, Tf, globulins, fibrinogen, and other specific proteins and molecules. From a speciation viewpoint, the serum constituents can be classified into two distinct groups, i.e., the LMM and HMM serum constituents, where the latter mostly comprise peptides and proteins.

The interactions between metal complexes and serum proteins such as HSA and Tf can have profound effects on absorption, distribution, metabolism, and excretion properties, and toxicity. In addition, the binding of a drug to these transfer proteins may affect targeted delivery, thereby increasing selectivity and decreasing the adverse effects. For example, binding to Tf can be advantageous for the cellular uptake of antitumor drugs via overexpressed Tf-receptors due to the higher iron demand of cancer cells, while the accumulation of HSA adducts is possible in inflamed tissues and tumors due to enhanced permeability and a retention effect.

HSA is the most abundant protein in human blood plasma, where it comprises about half of the serum protein content, with a typical concentration of 530–750 μM [119]. HSA maintains oncotic pressure, buffers pH, and transports thyroid and other mostly fat-soluble hormones, fatty acids, and unconjugated bilirubin, as well as many drugs. The serum albumin levels can affect the half-lifes of drugs [120]. HSA greatly augments the transport capacity of serum due to its high concentration and extraordinary binding capacity [121]. HSA has nonspecific binding pockets that can bind chemically diverse endogenous and exogenous compounds, where the principal sites are located in subdomains IIA, IIIA, and IB, which are often called sites I, II, and III, respectively [122].

Four types of metal ion-binding sites have been described: [123] the N-terminal binding site specific primary binds Cu(II) and Ni(II) ("ATCUN" = amino terminal Cu(II) and Ni(II)) [119,123]; the multi-metal binding site, which primarily binds Zn(II) and other bivalent metal ions [124]; site B is the primary binding site for Cd(II) but can also bind Zn(II) [123,125]; and the reduced thiol of Cys-34 binds gold and platinum compounds [123].

Transferrins are iron-binding blood plasma glycoproteins that control the level of free Fe(III) in biological fluids [126]. Tf comprises a polypeptide chain containing 679 AAs and two carbohydrate chains, with alpha helices and beta sheets that form two domains. The N- and C- terminal sequences are represented by globular lobes [127]. Tf contains two specific but remarkably similar high-affinity Fe(III) binding sites. Each lobe of Tf contains a distorted octahedral Fe(III)-binding site containing two Tyr, one His, one Asp, and one bidentate carbonate anion (the so-called "synergistic anion") [128]. Tf undergoes a conformational change when saturated by metal ions, where the C- and N-terminal parts move closer to each other and assume a closed conformation [5]. The serum concentration of Tf is ca. 37 μM and the saturation of Tf with Fe(III) is 15–50% [129], while it also binds efficiently to other metal ions such as Ga(III), Zn(II), V(III, IV, V), Al(III), Ru(III), and Bi(III) [130].

Immunoglobulins (Igs) are glycoproteins with the ability to react as part of the immune response to foreign bodies that are introduced or inoculated into an organism. Igs are divided into classes IgA, IgD, IgE, IgG, and IgM, which differ in terms of their biological properties, functional locations, and ability to react with different antigens. IgG is the most abundant class in the blood and it represents 75% of the total Igs. The IgG concentration in human blood serum is approximately 73 μM [131].

Alpha-2-macroglobulin (α2M) is one of the largest plasma proteins. In biological systems, it occurs mostly in a tetrameric form and its main function is the inhibition of proteases. A CysGlu fraction of the protein seems to play an active role in enzyme inhibition. However, the concentration of α2M is rather low in human serum, and thus its ability to bind metals is weak. With the exception of Zn(II), α2M has no role in metal ion transport in the serum [132].

4.2.3. Serum speciation by Al(III) and Fe(III) ions

Absorbed Al(III) is transported by the blood stream but its speciation in blood serum is still poorly understood. Most of the Al(III) is bound by the HMM iron transport protein Tf, and HSA and other potential HMM carrier serum proteins bind weakly to compete for a

significant amount of Al(III) [133]. Only citrate and phosphate are efficient binders among the LMM binders of serum. The somewhat contradictory speciation models are explained by the lack of reliable stability data for the complexes involved in the models and differences in the experimental conditions considered for speciation and modeling.

Harris et al. [134] used different UV spectroscopy, pH-potentiometry, and ESI-MS measurements to develop a model at an Al(III) concentration of ~10 μM, which is similar to the normal biologically relevant serum level (~0.1–0.3 μM) [135]. The speciation model provided in Table 6 of Ref. [32] suggests that 93% of the total Al(III) is bound to Tf. Among the pool of LMM aluminum, 88% of Al(III) will be bound to citrate, 8% to hydroxide, and ~2% to phosphate.

Table 6.

Speciation of Al(III) at pH ~7.4 and 25°C (based on data in Refs. [134, 136]).

	% of Al(III) bound	
	$c_{Al(III)}$ = 10 μM	$c_{Al(III)}$ = 1 mM
HMM components		
albumin	–	–
transferrin	93	77
LMM components		
phosphate	0.1	14
citrate	6	5
citrate-phosphate	2.8	4

In mM total Al(III) concentrations, which correspond better to aluminum overload conditions and those when the thermodynamic equilibrium is reached (monitored by multinuclear NMR; see later), the amount of phosphate-bound Al(III) increases significantly and ternary Al(III)-citrate-phosphate complexes can also be detected (see Table 6) [32].

The serum speciation of Fe(III) is simpler because it binds almost exclusively to Tf [66]. In healthy conditions, the LMM components have negligible importance. Citrate might be the only binder of Fe(III), which may be important [116]. The importance of Fe(III)-citrate in the serum may increase in iron overload conditions.

4.3. Chemical speciation in medicine

This section considers several examples of how the endogenous ligands present in various biological fluids and tissues influence the species distributions of biologically active medical drugs/prodrugs during absorption, distribution, metabolism, and excretion processes in the body.

4.3.1. Biospeciation of antidiabetic vanadium(IV, V) and zinc(II) complexes

Diabetes mellitus (DM), commonly known as diabetes, comprises a group of metabolic diseases where high blood sugar levels occur over a prolonged period. Diabetes is due to either the pancreas not producing sufficient insulin (type 1) or the cells in the body not responding correctly to the insulin produced (type 2). In 2015, it was estimated that 415 million people had diabetes worldwide [137], where type 2 DM (insulin resistance) comprised about 90% of the cases [138]. Type 1 diabetes can be treated with insulin, a natural peptide (protein) hormone made of 51 AAs, and over 40% of patients with type 2 diabetes require insulin injections as part of their treatment. However, insulin cannot be taken orally because it is degraded into fragments in the gastrointestinal tract (GI) so insulin is given as an injection in most cases [139]. Thus, this painful treatment needs to be replaced with an insulin "mimicker" that can be taken orally.

Surprisingly, many metal ions have insulin-like effects, such as Cr(III), Mn(II), Mo(VI), Se(V), V(IV/V), W(VI), and Zn(II). In particular, vanadium is one of the most efficient [140] and zinc is also biologically active at a higher dose by an order of magnitude [140, 141]. When it was originally discovered [142], $NaVO_3$ was shown to be toxic but many V(IV)O or even $V(V)O_2$ complexes have similar effects without toxicity [143]. Thus, it may be possible to improve the insulin mimetic/enhancing effect of vanadium salts using specific complexing agents. The orally administered vanadium complex should first enter the GI tract and pass into the blood serum, before arriving at the targeted cells. Biotransformation is possible throughout this process and the absorption efficacy from the GI tract can be improved by formulating the drug in an appropriate manner, including encapsulation [144]. However, the original carrier ligand can be replaced by serum/plasma components or endogenous binding molecules. The goal of modeling calculations for V(IV)O/V(V) and Zn(II) complexes in serum is to explore the potential biotransformation processes.

The V(IV)O [145-151], V(V) [152,153], and Zn(II) [154] complexes of drug candidate ligands and LMM serum constituents have been studied using several methods in a wide range of conditions, e.g., by pH-potentiometry in the pH range of 2–11, and complete speciation distributions of these multicomponent systems have been reported.

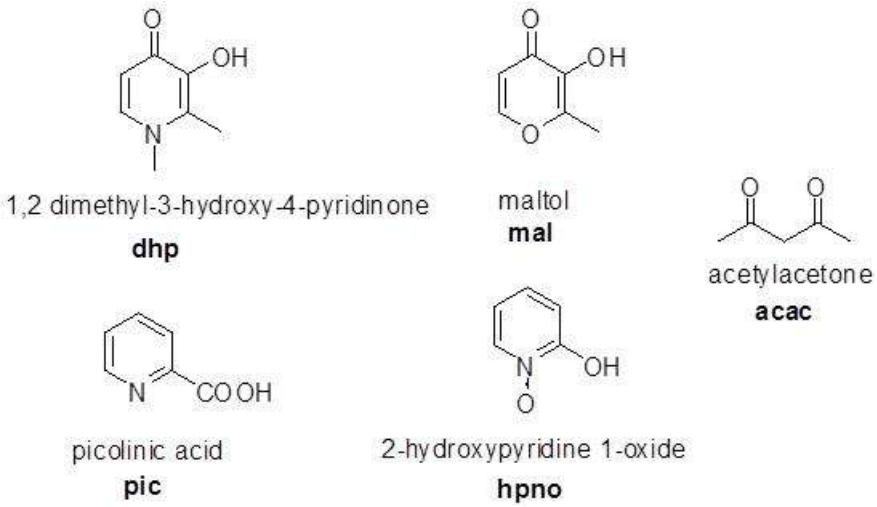

Fig. 5 Chemical structures, names, and abbreviations of several drug candidate ligands (in their neutral forms). All can form complexes with the composition $V(IV)OL_2$.

HMM serum protein speciation studies have focused on physiological pH conditions (7.4–7.5) and only conditional stability constants were obtained. Three of the HMM serum components, i.e., apotransferrin (apoTf), HSA, and Igs, have been studied using different methods (see Sections 4.3.1.1–4.3.1.2).

4.3.1.1. Interactions of V(IV)O and V(V) with transferrin

V(V)O binds at the two iron-binding sites and similar to Fe(III), only in the presence of HCO_3^-. However, the X-band EPR of V(IV)O–apoTf complexes indicates that there are two different (A and B) coordination environments for V(IV)O at physiological pH, and these differences have been described previously [68]. The stability constants of the V(IV)O-apoTf complexes are sufficiently high but they cannot be determined directly at physiological pH because the complex formation is actually complete (100%). The free V(IV)O is hydrolyzed at pH 7.4 and the composition and stability of the hydroxido complexes formed are not known fully, so metal ion competition is not suitable option for accurate determination. Thus, the ligand competition method is the only option for obtaining the binding constants. Similar conditional stability constants ($\log \beta'_1 = 13.0–13.4$ and $\log \beta'_2 = 25.2–25.5$) [33, 155] were

determined by two different groups using four different competitive ligands: nitrilotriacetic acid (nta), dhp/mal, and acac, and with various measurement techniques (UV-Vis, CD, and EPR spectroscopy). dhp, mal, and acac are drug candidate ligands. Ternary complex formation by dhp/mal makes their quantitative description more difficult, where both lobes of apoTf can bind a V(IV)O(mal) or V(IV)O(dhp) unit and the coordination environment is probably uniform. The almost significant difference between the calculated log K_1 and log K_2 values (based on statistical considerations, logK_1–log K_2 = log (K_1/K_2) must be 0.6 if the two binding positions are equal; see Ref. 8) is in agreement with the spectroscopic observations. Mal forms less stable ternary species than dhp and similarly, V(IV)O$(mal)_2$ is less stable than V(IV)O$(dhp)_2$. Formation of the ternary complex with dhp is noncompetitive according to the concentration of HCO_3^-, where in the absence of the synergistic anion (HCO_3^-), ternary complex formation with dhp is less favored. In fact, a quaternary species has been found: V(IV)O – apoTf – HCO_3^- – dhp. Thus, the determined stability constants are valid only at pH 7.5 and a HCO_3^- concentration of 25 mM [33] (another ternary complex with dhp has also been assigned with a different 1:1:2 V(IV)O-Tf-dhp composition [69]). Ternary complex formation was observed with picolinic acid (another drug candidate ligand) lactate (serum constituent) and picolinic acid is considered to behave as a synergistic anion [69].

The conditional stability constants of the V(V)-apoTf complexes (log β'_1 = 6.0 and log β'_2 = 11.4) were determined by ^{51}V-NMR spectroscopy and ultrafiltration, and no competition was found between V(V) and HCO_3^- for the anion-binding positions of apoTf [152].

4.3.1.2. Interaction of V(IV)O with human serum albumin

HSA can bind V(IV)O at two independent and different binding sites at least. CD spectroscopic studies indicate that vanadium binds (at least partly) as a monomer at the ATCUN site and as an EPR silent dinuclear species at the multi-metal binding site. CD spectroscopic measurements have confirmed these EPR findings. The stability constants for (V(IV)O)HSA (log β' = 9.1) and $(V(IV)O)_2$HSA (log β' = 20.6–20.9) species were determined in liquid nitrogen temperature and room temperature EPR experiments by two different research groups [156, 157]. Ternary complex formation (HSA$(V(IV)O_2(L_2)_n)$ with several carrier ligands (dhp, maltol, hpno, pic) has been described quantitatively. In these bis-ligand complexes the metal ion is coordinated via a surface His side-chain of the protein, which binds in the equatorial position to the *cis* form (with the coordinated water *cis* to the oxido-O atom) of the bis ligand V(IV)O complexes [69]. In the case of the $VO(acac)_2$ complex, no

ternary complex formation is observed with HSA. The stability constant of cis-$V(IV)O(dhp)_2HSA$ is log K′ = 25.9 [155].

The complexation strength of IgG to VO(IV) is about the same as that of HSA (log β′ = 10.3 [158]), where it can also bind and carry bis-complexes such as $V(IV)O(pic)_2$.

4.3.1.3. Speciation of VO(IV) in blood serum

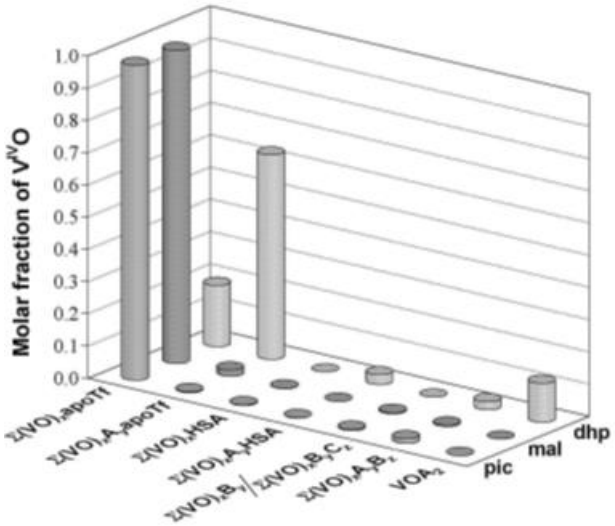

Fig. 6 Speciation of various potentially antidiabetic VO(IV) compounds (10 μM) in serum at pH 7.4. The summed concentrations of similar species types are depicted: VOA_2: VO(IV) bound in the binary bis complex, $(VO)_xB_y$: binary species formed with the LMM components of the serum, $(VO)_xB_yC_z$: ternary species of the LMM components of the serum, $(VO)_xA_yB_z$: ternary species of an antidiabetic complex with LMM components of the serum, $(VO)_x$apoTf: binary species of VO(IV) with apoTf, $(VO)_xA_y$apoTf: ternary species of an antidiabetic complex with apoTf, $(VO)_x$HSA: binary species of VO(IV) formed with HSA, and $(VO)_xA_y$HSA: ternary species of an antidiabetic complex with HSA. A: carrier ligands, pic, mal, and dhp; B and C: LMM components of the serum: citric acid, lactic acid, and phosphate. Taken from Ref. [159].

The speciation of the metal ion among the LMM and HMM components of blood serum, and the original metal ion carrier ligands, including mixed ligand species, was calculated based on the stability constants and concentration data, and the results are summarized in Fig. 6. The results show clearly that: (i) Tf, one of the two important HMM binders, is much more efficient than HSA and it can displace 30–70% of the original carrier from the complex, or form ternary complexes with them; (ii) only the hydroxypyridinone

derivative dhp is a sufficiently strong carrier to preserve a significant proportion of the VO(IV) in the original complex (in the free form or bound to Tf), whereas in other cases, the carrier ligands are displaced by serum components; (iii) among the LMM binders, citrate is the only "active" component that can influence the solution state of these antidiabetics. These results have been confirmed by native blood serum measurements obtained using ultrafiltration, followed by separation through a 10-kDa membrane, where the LMM and HMM fraction-bound VO(IV) levels were measured by atomic absorption spectrometry [33,160]. Similarly, the protein-bound VO(IV) was separated by anion exchange chromatography and determined by ICP-MS. Only Tf can bind V(IV)O and the binding ability of the other serum protein (HSA) is negligible [33]. Thus, the most important role of the carrier ligand seems to be facilitating the absorption of VO(IV) from the GI tract, but the complexes finally fall apart in the serum. Pharmacokinetic investigations [161] have supported these predictions using labeled [*bis*(maltolato)oxovanadium(IV)] complexes.

However, it should be mentioned that higher concentrations of the V(IV)O complexes, e.g., mM level, which may exceed the concentration of the strongest V(IV)O binder protein Tf, mean that HSA can also be an important binder of V(IV)O species due to its significantly higher concentration in serum [159].

Clearly, all thermodynamic models have their limitations because there are actually no static equilibria in living systems. Furthermore, it would be difficult to perform calculations for the whole blood, such as including the cells in the plasma. However, X-ray absorption near edge structure (XANES) studies [162] suggest that red blood cells also have an important role in the biospeciation of vanadium.

4.3.2. Speciation of V(V) in blood serum

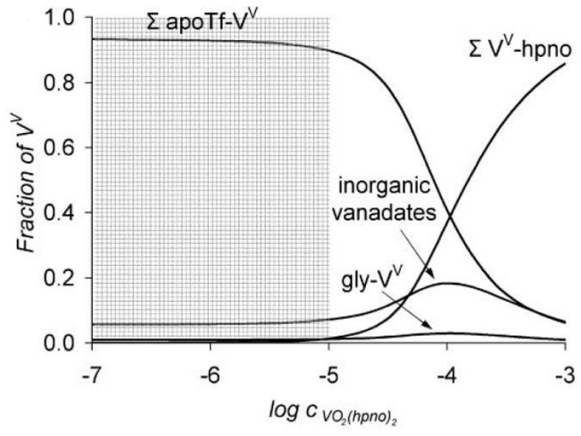

Fig. 7 Calculated speciation of $[VO_2(hpno)_2]^-$ in blood serum. Taken from Ref. [152]

Among the various drug candidate ligands, hpno forms the most stable complex with V(V) at pH 7.4. The conditional stability constant (log β′) values for maltol and dhp complexes under the same conditions are ~0.6 units lower.

The stability constants determined by ^{51}V-NMR spectroscopy and ultrafiltration for the V(V)-apoTf interaction are in very good agreement. The predicted speciation of $[VO_2(hpno)_2]^-$ is depicted in Fig. 7, which shows clearly that at biologically relevant concentrations, i.e., c(V(V)) < 1 × 10^{-5}M, Tf is the only V(V) binder in the blood serum. Under these concentration conditions, the carrier ligands, HSA, or small biomolecules present in the serum (lactate, citrate, phosphate, Gly, or His) do not form sufficiently strong complexes to compete with apoTf, although ~5% of the V(V) exists as free $H_2VO_4^-$ ions in solution [152].

The dipicolinate complex of vanadate has also been studied extensively [163], where specific studies have been performed with monolayers and reverse micelles [164], unfortunately it mostly decomposes in the serum at pH 7.4 [165].

4.3.3. Speciation of Zn(II) in blood serum

Zinc(II) is not as efficient as vanadium at insulin mimesis, but it is an essential element and it may be accepted more easily as a medical drug. Studies have been performed with some zinc(II) complexes that exhibit insulin-like activities at concentrations of ca. 100 μM level [159]. The potential interactions of drug candidate complexes in the serum with LMM components have been studied in detail by pH-potentiometry [34, 70] based on modeling calculations of these binders (without the HMM components) with His and Cys, and their ternary complexes as primary Zn(II) binders.

HSA binds Zn(II) with conditional binding constants in the range of log K′ = 7.1–7.9 [166, 167]. α2M also has considerable Zn(II) binding properties, but it is present at a much lower concentration in the blood serum than albumin (2–6 μM), with conditional formation constants of log K'_1 = 7.49 and log K'_2 = 5.12 [168-171]. The third possible Zn(II) binder is Tf, where the Zn(II) binding constants are log K'_1 = 7.8 and log K'_2 = 6.4 (15 mM $NaHCO_3$) [172,173]

If both the HMM and the LMM serum binders are considered together, then modeling calculations indicate that most of the total serum Zn(II) is bound to the serum proteins

(~98%), where HSA is the primary binder (80–90%) [29,34,169,173] followed by α2M (5–15%) [169-171]. However, the role of apoTf is still under discussion [170,173] and it has been reported that a minority of Zn(II) circulates unbound or attached to LMM components in blood serum.

Human serum samples have been incubated with Zn(II) compounds to study the binding behavior of Zn(II) complexes with serum components under more realistic conditions. CZE experiments with ICP-MS detection were used to identify the metal ion in different serum components, which showed that most of the Zn(II) was bound to HSA (~80–95%) according to the ^{34}S trace. A minor amount (<5%) of Zn(II) was still coordinated with the original carrier (or other buffer components), but no Zn(II) was bound by Tf [34]. Thus, the results of modeling calculations (see above) were confirmed experimentally by CZE-ICP-MS and by ultrafiltration-ICP-atomic emission spectroscopy [70] studies.

4.4. Biospeciation of anticancer metal complexes in blood serum

Most of the antitumor metal complexes are administered intravenously, such as Pt(II)-containing drugs (cisplatin, carboplatin, and oxaliplatin) or clinically investigated Ru(III) compounds (*vide infra*), and serum proteins are the first and most important available biological binding partners when they enter the bloodstream.

Based on their enhanced permeability and retention due to the accumulation of HSA in tumor tissues, Pt(IV) prodrugs were designed to bind non-covalently to native HSA by Lippard et al. [174], and thus the controlled release of these compounds is possible in disease areas [175,176]. Maleimide-functionalized compounds have also been developed (including Pt(IV) complexes [177]) that can bind covalently to the free thiol group of HSA (Cys34), although a cleavable specific bond between the drug and maleimide moieties is beneficial in these cases, e.g., an acidic environment sensitive linker [176]. Fairly diverse binding events are possible in terms of the serum protein-binding modes and reaction rates in the case of metallodrugs. Binding via non-covalent bonds (such as hydrogen and salt-bridge bonding, π-π stacking interactions, and Van der Waals force) does not change the coordination mode and thus the complex retains its original entity. It can be concluded that non-covalent and weak to moderately strong reversible binding to HSA might be advantageous for targeted delivery. By contrast, irreversible and strong binding, which generally occurs via coordinative bonds accompanied by partial or complete displacement of the original ligand(s) by the donor atoms of the protein, may lead to the inactivation of metal complexes, especially in slow ligand-

exchange processes. Thus, the complex cannot reach the desired site of action and the formation of covalent metallodrug-protein adducts might be responsible for side effects in chemotherapy.

Therefore, obtaining deeper insights into the rate, strength, and the nature of the binding between a metallodrug and serum proteins is crucial for understanding their pharmacokinetic properties, transport, and mechanisms of action. In order to characterize the reaction rates of metallodrug-protein interactions, the formation constants as well as the number and localization of the binding sites are available based on a wide variety of conventional and advanced analytical techniques [178]. An advantage of spectroscopic methods, such as NMR, fluorescence, UV-Vis, CD, X-ray absorption, XANES, EPR, electron nuclear double resonance (ENDOR), is that these are non-invasive techniques and the chemical equilibrium is not shifted by their application, so they are highly recommended for determining binding constants. Various MS methods can be combined with fragmentation experiments to probe binding and obtain information about the stoichiometry of protein adducts as well as their binding sites. Separation techniques such as ultrafiltration and capillary electrophoresis, HPLC, size exclusion chromatography-MS, and ICP-MS have been used widely to study the distribution between free and protein-bound forms, or between different blood compartments [178,179]. These separation methods are appropriate for investigating the distributions in biological fluids and tissues, as well as using serum samples obtained from treated cancer patients or animal models.

The role of LMM compounds in the serum is not negligible because they may be responsible for the (partial) displacement of the original ligand, or the formation of ternary complexes, where serum reductants (e.g., ascorbate) may reduce the metal center. In particular, chloride ions are often considered to be coordinating ligands (Pt(II), Ru(III), and Rh(III)), which can influence the aquation and hydrolysis of metal complexes [180]. Analyses of samples from *in vivo* treated animals or patients have unambiguously demonstrated the key roles of serum proteins in the distribution of numerous antitumor metallodrugs. For example, the Ru(III) complex NKP-1339 binds with HSA as the major serum binder, where rapid non-covalent binding to this protein protects the complex against reduction and hydrolysis, which may contribute to the low frequency of side effects observed in clinical trials (see Section 4.6.5). The slow formation of covalent bonds was also observed. However, the adverse effects of cisplatin are related to reactions between the drug and serum compounds, specifically proteins and S-containing peptides. Cisplatin predominantly binds to HSA in real-world samples, although the concentration of the free drug is highly dependent on time (up to 90%

of Pt(II) is bound to proteins at 3 h after infusion) [180]. Most of the Pt(II) is covalently bound and the coordination of the protein donor atoms (and thus the exchange of the original ligand(s)) is slow due to the kinetically more inert feature of the metal ion. The protein binding profile is different for the three Pt(II) drugs, where the level of protein binding is the lowest for carboplatin, and oxaliplatin preserves its original form most poorly in the unbound fraction [180,181]. Protein binding occurs slowly in the unbound fraction so the Pt(II) complexes are affected by various transformation processes such as aquation (Cl^-/H_2O exchange, cisplatin), oxalate chain loosening (oxaliplatin), and reactions with small peptides (glutathione (GSH)) and AAs (Cys, Met) [180], which are also time-dependent processes. Unfortunately, comparative binding data are not available for the HSA adducts of the three Pt(II) complexes, although large variations have been reported regarding the number of binding sites (up to 5–12) and binding constants [178,180,182,183] for the "old" drug cisplatin. The major binding site of cisplatin on HSA probably involves a (S(Met298),N) macrochelate [183], and $\log K'_{HSA}$ = 3.88 and 4.17 were reported for cisplatin and oxaliplatin, respectively, by Rudnev et al. [182]. Thus, estimating the distribution in such complex systems would be difficult under non-equilibrium conditions.

By contrast, for the kinetically more labile Ga(III) complexes, the serum distribution can be modeled mathematically using stability data. Numerous Ga(III) complexes have been developed as antitumor agents, where *tris*(8-quinolinolato)gallium(III) (KP46) and *tris*(maltolato)gallium(III) (GaM) are the most promising orally active agents that are currently undergoing clinical trials. The serum distributions were computed for KP46 and GaM complexes based on their solution stability and interactions with serum components. Despite the structural similarities of these Ga(III) complexes, KP46 has a stability constant that is about eight orders of magnitude higher than that of GaM, with much higher lipophilicity [43]. These features have major effects on their binding processes with serum proteins [35]. GaM does not bind to HSA, but moderate binding between KP46 and HSA via non-covalent bond while retaining the coordination environment around the metal ion was demonstrated ($\log K' = 4.04$) based on fluorometric and saturation transfer difference NMR measurements. The binding of KP46 with the protein occurs via the IB binding site according to modeling calculations. Tf can compete for Ga(III) with the carrier ligands of the complexes, but substitution by maltol occurs to a much higher extent compared with that by 8-quinolinol. Based on these findings, equilibrium modeling calculations of the biospeciation of KP46 and GaM were performed for Ga(III)–ligand–HSA–Tf systems. The stability constants of the following species were used in the calculations: associates present in the

Ga(III)–ligand systems (GaL, GaL_2, GaL_3, HL, H_2L, and $Ga(OH)_{i=1–4}$), KP46-HSA and maltol-HSA adducts, and Ga(III) complexes of Tf (GaTf, Ga_2Tf). The effect of the LMM components on the distribution was negligible. Unambiguously different distributions were obtained for KP46 and GaM. Tf has a significant role in the case of GaM and the protein can replace maltol completely at concentrations lower than 30 μM. By contrast, the binding of KP46 to HSA is estimated under physiologically relevant conditions (Figure 8.). The binding of KP46 to HSA is reversible and does not alter the original coordination mode of the complex, which might increase its solubility and half-life. This finding also suggests a Tf-independent gallium uptake mechanism for KP46 [35].

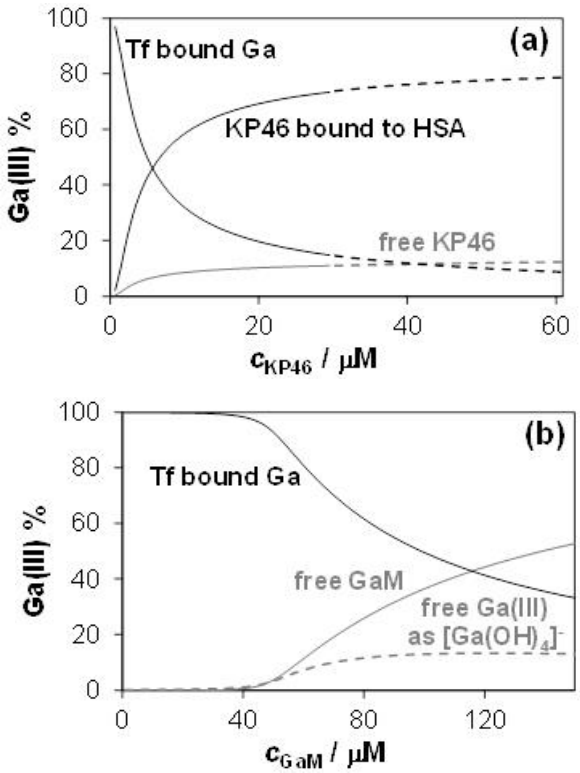

Fig. 8 Concentration distribution curves for the Ga(III) complex–HSA–Tf systems as a function of the analytical concentrations of the complex for KP46 (a) and GaM (b). Dashed lines denote the KP46 concentration range over the solubility limit. (pH = 7.4; c_{HSA} = 630 μM, c_{Tf} = 37 μM considering that 30% of the binding sites of Tf are saturated with Fe(III)) Adapted from Ref. [35]

Therefore, in addition to investigating the reaction rate, the extent of binding (determination of binding constants when an equilibrium is reached) and the nature of the binding event (non-covalent/coordinative) are important for successful drug development.

4.5. Speciation investigations with a magnetic resonance imaging (MRI) contrast agent

MRI is a medical imaging technique used for diagnosis by imaging the anatomy and physiological processes in the body. MRI has a wide range of applications in medical diagnosis and over 25,000 scanners are estimated to be in use worldwide [184]. MRI is based on NMR, where the most frequently studied nucleus is ^{1}H. By varying the parameters of the pulse sequence, different contrasts can be generated between tissues due to the relaxation properties of the hydrogen atoms present. A contrast agent usually shortens, or in some cases increases, the value of T_1 (spin-lattice relaxation time) for nearby water protons, thereby altering the contrast of the image [185]. Around 30–40% of clinical MRI applications use paramagnetic complexes (or superparamagnetic, ferromagnetic substances) as contrast agents [186]. The trivalent Gd(III) is the most efficient relaxation agent among all the paramagnetic cations due to its high electron spin (S = 7/2) and slow electron spin relaxation. Other paramagnetic metal ions have also been considered as MRI contrast agents, particularly the non-toxic biocompatible manganese(II) (S = 5/2) [187].

The free Gd(III) ion is toxic [188] so it must be chelated with appropriate multidentate ligands, which ensure high thermodynamic stability and/or kinetic inertness. The majority of clinical Gd(III)-based agents, which represent around 90% of all clinical contrast agent injections, have low molecular weight, an extracellular space localization, and they are non-specific [186]. At present, nine different Gd(III)-aminopolycarboxylate complexes are used in clinics, which are mainly derivatives of the open chain H_5DTPA (diethylenetriaminepentaacetic acid) or the macrocyclic H_4DOTA (1,4,7,10-tetraazacyclododecane-1,4,7,10-tetraacetic acid) [189,190] (Fig. 9).

The increasing clinical use of Gd(III)-based contrast agents was halted in 2006 when the development of a newly observed disease called nephrogenic systemic fibrosis (NSF) was assumed to be related to the use of Gd(III) [191,192]. NSF is a very rare, highly debilitating, life-threatening disease, which was observed only in patients with severe or end-stage renal disease [191-198]. The number of NSF cases reported by the end of 2007 was around 400, but due to the recommendations of health authorities, the number of cases decreased dramatically

and no new cases have been reported [194,199,200]. About 75–80% of the known NSF cases could be associated with the use of Omniscan ([Gd(DTPA-BMA)], where BMA = *bis*-(methylamide)) whereas far fewer disease have been reported in patients treated with Magnevist ([Gd(DTPA)]), and only a few cases have been observed after the use of macrocyclic agents [191,198,201-205].

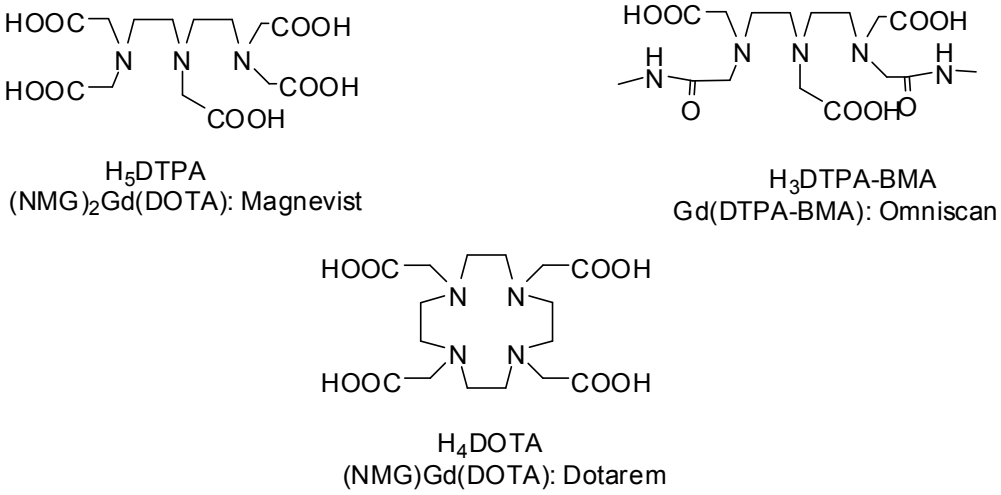

Fig. 9 Chemical structures of ligands, formulae, and trade names of Gd(III) complexes used as contrast agents (NMG: N-methylglucosamine).

In body fluids, many metal ions and ligands may compete with the Gd(III) ion and the DTPA-BMA^{3-} ligand, respectively. Equilibrium calculations have been performed using a simplified plasma model including the Cu(II)/Zn(II)/Ca(II) cations, AAs (Ala, Cys, Glu, Gly, His, and Lys), HSA, Tf, and small biomolecules (carbonate, phosphate, citrate, lactate, malate, and succinate) [206]. The model predicted that under physiological conditions (pH = 7.4; t = 37°C; I = 0.15 NaCl), the phosphate ion is the only endogenous ligand that can compete with DTPA-BMA^{3-}. Approximately 17% of the [Gd(DTPA-BMA)] dissociates to form Gd(PO_4) as a precipitate. The ligand DTPA-BMA is also released and it can form complexes with endogenous metal ions, so Zn(II), Cu(II), and Ca(II) ions may form complexes. Due to the relatively high concentration of the contrast agent (0.35 mM), the free DTPA-BMA can collect approximately ~80% of the serum Zn(II) and ~90% of the Cu(II) [206].

However, the dissociation of [Gd(DTPA-BMA)] in human serum is controlled kinetically rather than thermodynamically. The dissociation of the complex occurs alongside its elimination from the body, where the amount of Gd(III) released from [Gd(DTPA-BMA)]

in body fluids depends on the rate of dissociation and elimination of the complex. An open two-compartment model was developed to assess the amounts of Gd(III) released in body fluids based on rate data obtained from pharmacokinetic studies of the elimination of [Gd(DTPA-BMA)] and rate data characterizing the dissociation of the Gd(III) complex.

In patients with normal renal function, rate data indicate the elimination of about 95% of the administered [Gd(DTPA-BMA)] within about 48 h. In patients with severe renal impairment, the elimination of [Gd(DTPA-BMA)] is slow ($t_{1/2}$ ~30–40 h) and during the long residence period, large amounts of the complex may dissociate so significant amounts of Gd(III) (approximately 12.5% in 5 days after the administration) can be deposited in the body [206].

4.6. Kinetic aspects of speciation in biology

In terms of trace element speciation, in addition to thermodynamic stability, kinetic factors strongly affect the occurrence of species in a biological system, organ, organ compartment, etc. The ligand exchange reactions of different metal ions are variable and their rate is influenced greatly by the chemical environment where the metal ion occurs. The following general rule is valid for the lability of metal ions bound in various chemical forms in biological systems: aqua ions > inorganic ligands > LMM > HMM. The mobility of metal ions may also depend on their oxidation state. For example, chromium with an oxidation state of six has high mobility and relatively fast absorption, whereas it is one of the most inert transition metal ions with an oxidation state of three. Chromium is sold in drug stores as a nutrient and it leaves the body in the same form consumed due to its extreme inertness. However, if a small proportion is reduced to an oxidation state of two, then it catalyzes the ligand exchange reaction and the chromium might be absorbed, although there is no sufficiently strong reducing agent in the body that can reduce Cr(III) to Cr(II). The next sections provide a few examples where the different rates of various reactions in biological milieu cause significant changes in the speciation of biological fluids or tissues.

4.6.1. Speciation of Al(III) in blood serum: citrate vs. phosphate

As discussed above, the slow formation of oligomeric species of Al(III) with some LMM components can lead to uncertainty regarding the serum distribution of Al(III) [133]. According to NMR, Al(III) readily forms mononuclear mono and bis complexes where after

mixing, the components oligomerize into a trinuclear complex in a rather slow process [207]. Furthermore, if phosphate is also present, ternary species predominate throughout the whole pH range from mixing until the actual thermodynamic equilibrium is reached. Time only affects the concentration of the trinuclear species, which is formed in a rather slow process from the mononuclear species [208]. Interestingly, if phosphate is added to this solution at least in a twofold excess, the monodentate phosphate can displace the tridentate citrate from the oligomeric complex over a longer period, where the characteristic quartet of the free citrate is present in the ^{1}H NMR spectrum (Fig. 10) [208].

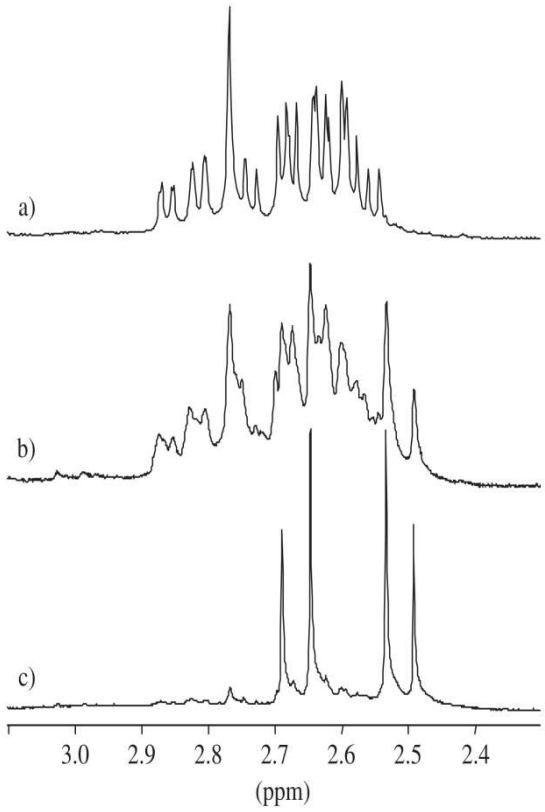

Fig. 10 ^{1}H NMR spectra recorded during the decomposition of the trinuclear Al(III)-citrate complex at pH 7.4. Spectrum of the trinuclear species $[Al_3(citrateH_{-1})_3(OH)]^{4-}$ at 10 mM (a), 10 h (b), and 5 days (c) after adding a twofold excess of phosphate. Adapted from Ref. [208].

Modeling calculations have shown that at thermodynamic equilibrium, phosphate seems to be the most efficient binder of Al(III) (75%) in serum, although citrate-bound Al(III) also occurs at a significant concentration (20%), [208] which was confirmed by Bell et al. [209] who detected Al-bound citrate in native serum by ^{1}H NMR, whereas the remainder was

present in the ternary species. Similarly, Bantan et al. investigated the speciation of LMM Al(III) complexes in human serum by liquid chromatography and ESI-MS. In agreement with the results described above, they found three main Al(III) species present in serum: Al(III)-citrate, Al(III)-phosphate, and the ternary Al(III)-citrate-phosphate [210].

In a more elegant manner, a computer-assisted real-time model was used by Beardmore and Exley to describe the distribution of sluggish metal ions in biological systems, such as Al(III) in serum [211]. As shown in Fig. 11, their model basically agrees with the semi-quantitative treatment discussed above, where LMM citrate is another important binder as well as Tf during the whole period after the addition of Al(III). Their model also predicted a significant role for the formation of an aluminum hydroxide phase, which was substituted in the other model by a phosphate-hydroxido ternary $Al(III)BH_{-1}$ ($Al(III)PO_4(OH)$) phase. In addition, it should be mentioned that this other model omitted the pH and time ranges when the precipitation of solid materials occurs in the system.

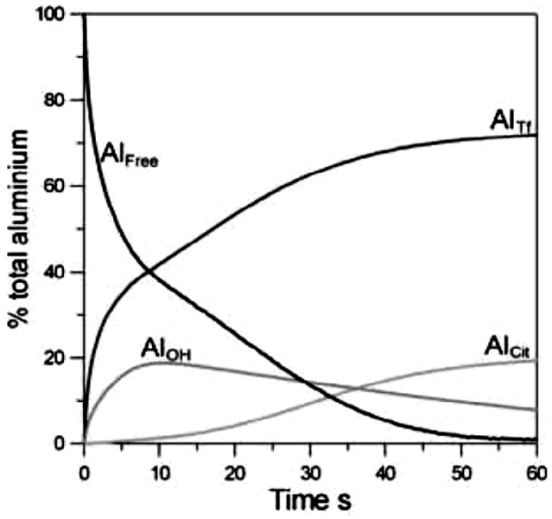

Fig. 11 Distribution of Al(III) between blood serum components as a function of time. Adapted from Ref. [211].

4.6.2. Speciation of Ca(II) in saliva

This example considers some quantitative details regarding the demineralization-remineralization equilibrium of tooth enamel [212]. Saliva is a complex biofluid, which contains inorganic anions, cations, nonelectrolytes, AAs, proteins, carbohydrates, and lipids. The pH of saliva is close to neutral in the absence of dietary acids.

The major inorganic component of tooth enamel is hydroxyapatite (HAP; $Ca_5(PO_4)_3(OH)$). Several other types of calcium phosphates may also precipitate in the mouth, including tricalcium phosphate (TCP; $Ca_3(PO_4)_2$), tetracalcium phosphate ($Ca_4H(PO_4)_3$), and calcium hydrogenphosphate (CP; $CaHPO_4$). If fluoride is present, the demineralization–remineralization equilibrium is influenced greatly by the formation of fluoroapatite (FAP; $Ca_5(PO_4)_3F$), which has much lower solubility and thus it is formed in the remineralization process. Saliva continuously provides calcium and phosphate to the surfaces of the teeth at concentrations that cannot inhibit the demineralization caused by acids in dental plaque (but that also facilitate some remineralization), or at least halt the early stages of carious lesion formation (enamel demineralization). Table 7 shows the major calcium species in saliva [212].

Table 7

Predicted Ca(II) phosphate species at various pH values in saliva based on model calculations (based on data in Refs. [212-214]).[a]

pH	long-term model	short-term model
5.00	FAP	Ca^{2+} and $Ca(citrate)^-$
6.00	FAP and HAP	Ca^{2+} and $Ca(citrate)^-$
6.75	FAP and HAP	TCP and CP
7.00	FAP and HAP	TCP and CP

[a] Abbreviations in the table, FAP: $Ca_5(PO_4)_3F$, HAP: $Ca_5(PO_4)_3(OH)$, TCP: $Ca_3(PO_4)_2$, CP: $CaHPO_4$.

The thermodynamically most stable apatites form slowly from more readily precipitated precursors, so the model that includes apatites is called the long-term model, whereas the other without HAP and FAP is called the short-term model. The former may be considered as an equilibrium model of the system, whereas kinetic factors inhibit the direct formation of apatites in the latter. Computer modeling calculations suggest that CP and TCP are the most likely precursors of HAP.

4.6.3. Interactions of Pd(II) complexes with nucleotides and thioether ligands

Numerous Pt(II) complexes are used widely as anticancer agents, where their antitumor activity is related to the platination of DNA by interacting with guanine bases. However, it is also clear that platinum-sulfur interactions may also play significant roles in both the transport

and nephrotoxicity of Pt(II)-containing agents. Previous studies of thioether and nucleobase complexes of Pt(II) demonstrate that the two types of donor sites are opposed in terms of their kinetic and thermodynamic behavior. The thioether adducts form relatively rapidly, which results in the formation of various metastable species, whereas they are readily substituted by various nitrogen donors in the equilibrium state. However, the very slow formation kinetics of Pt(II) complexes make it very difficult to describe these systems. Thus, Sóvágó et al. [215] used the corresponding Pd(II) systems to study the time-dependence of metal ion speciation, where they determined the thermodynamics and kinetics of PdL complexes with monodentate N-alkyl nucleobases (N) and thioether ligands (S). In PdL, L denotes a tridentate chelating agent, diethylenetriamine (dien) or terpyridine (terpy), which form very stable complexes with Pd(II) and leave a single coordination position empty around the metal ion, thereby allowing further substitution. Ternary complexes of the N donors have thermodynamic stability constants that are about three orders of magnitude higher than those of the thioether complexes, but the rate constants of the substitution reactions show that the formation of thioether complexes is faster by at least a factor of 10 [216-218]. The combined application of thermodynamic and kinetic parameters yielded the time-dependent speciation process shown in Fig 12.

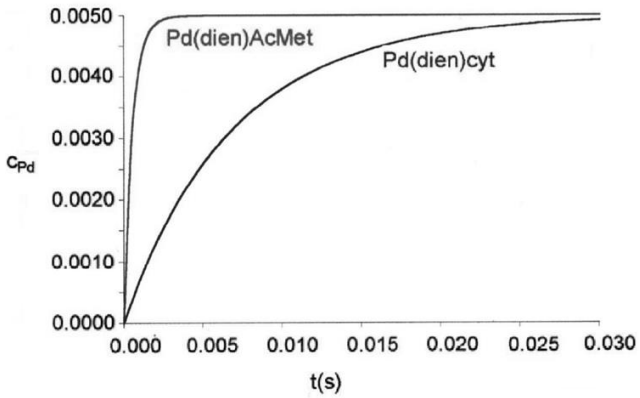

Fig. 12 Concentration of thioether- and nitrogen-bonded adducts as a function of time in binary systems obtained by mixing Pd(dien) and acetyl-methionine (AcMet) or cytidine (cyt) at a ratio of 1:2. Adapted from Ref. [215]

The thermodynamic equilibrium state of this multicomponent system is characterized by the coordination of N-donors, which supports the assumption that the Pt-S bonds formed by platinum anticancer agents can play roles in the transport and toxicity of platinum drugs. These findings and the relative ratio of the ligand exchange rate constants for Pd(II) and Pt(II)

($\sim 10^5$) indicate that the maximum formation of Pt-S bonded species should occur within a few hours, whereas the equilibrium should require a few months. It is unclear where the Pt(II) compounds will be located such a long period after administration. These results are not very promising in terms of the actual speciation of anticancer Pt(II) compounds in biology, and thus their efficacy.

4.6.4. Transport of Cu(II) from complexes with His-containing peptides to Cys

Cu transport in the blood has been studied extensively [219,220], where ^{64}Cu isotope experiments have shown that most of the Cu bound to ceruloplasmin is not exchangeable, whereas that bound to HSA is exchangeable with LMM Cu carriers, such as AAs. The resulting complexes formed with AAs are considered important as Cu carriers through membranes (Eq. 5) [221].

$$\text{Cu(II)-HSA} + \text{AA} \leftrightarrow \text{Cu(II)-HSA-AA} \leftrightarrow \text{Cu(AA)}_2 \leftrightarrow \text{membrane Cu(I) species} \quad (5)$$

Recent findings have greatly improved our understanding of Cu transport in cells. In particular, studies of many intracellular Cu proteins, e.g., Cu-MRI, have clarified the relationships between Cu transport and different genetic disorders such as Menkes disease [222]. These studies demonstrate that in addition to passive transport, other pathways through the membrane might involve ATPase. The Cu form inside cells is Cu(I), whereas that outside cells is Cu(II). The conversion mechanism involving a redox reaction remains unclear, but Cu(II) is assumed to be reduced by a thiol compound, such as Cys, GSH, or a Cu transport protein. Reduction is the force that drives Cu into the cell, so its speciation and mechanism are important for understanding Cu transport through membranes.

Cu(II) is bound to HSA by the N-terminal moiety in a 4N (NH_2, 2×amide-N^-, imidazole-N) manner, where it forms a stable complex with λ_{max} in a similar manner to Cu(II)-GlyGlyHis [223]. Thus, His-containing tripeptides provide a good model of HSA binding to Cu(II). Kinetic studies of various peptides with Cys using stopped flow methods determined the following reaction path (Eq. 6) [224].

$$\text{Cu(II)-peptide} + \text{AA} \leftrightarrow \text{Cu(II)-peptide-Cys} \leftrightarrow \text{Cu(II)(Cys)}_2 \leftrightarrow \text{Cu(I) species} \quad (6)$$

This reaction is similar to the ligand substitution reaction (Eq. 5), but the Cu(I) complex is formed in solution. Before the reduction of Cu(II), the formation of the ternary complex can be used to obtain information about Cu transport. For the Cu(II)-GlyGlyGly $CuLH_{-2}$ complex, Cys-SH first attacks the carboxylate site (the fourth coordination site of $CuH_{-2}L$) and Cys is bound in a monodentate manner in the ternary complex $CuLH_{-2}Cys$ [49]. For the Cu(II)-GlyGlyGly system, the ternary complex forms rapidly, but a brief decrease in ternary complex formation can be observed based on the spectra as the reaction proceeds (Eq. 6). Surprisingly, in the presence of Cys, the Cu(II)–GlyGlyHis complex has the spectrum of the binary complex and the spectrum of the ternary complex is not observed [225]. This is due to the relatively slow formation of the ternary complex and because Cu(II) changes rapidly into the Cu(I) species (see Fig. 13.)

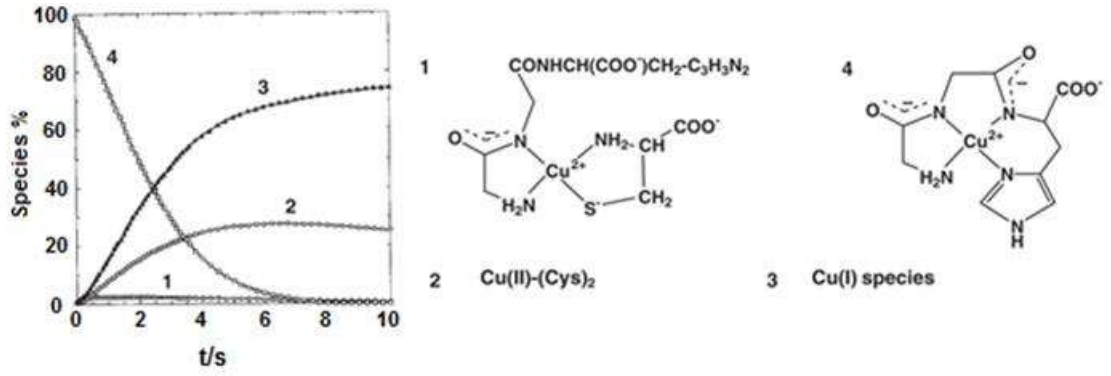

Fig. 13 Time-dependent distribution of the Cu species formed during the reaction of [Cu(GlyGlyHisH_{-2})] with Cys at pH 8.7. Adapted from Ref. [226].

The slow ternary complex formation can be attributed to the strong Cu(II)-imidazole bond at the fourth coordination site, which stabilizes the two amide-N- bonds. The kinetic constants for the reaction from the ternary complex to Cu(I) are similar for each system that has been studied. The pH-dependence of the kinetic constant for ternary complex formation suggests that formation of the adduct occurs with concomitant H^+ transfer. H^+ uptake by the deprotonated peptide bond to obtain $CuLH_{-1}Cys$ is probably the limiting factor. In the case of GlyGlyHis, the $CuH_{-2}L$ complex is considered to be a poor H^+ acceptor, because the two amide-N units are stabilized by two strong anchor donors, i.e., NH_2 and imidazole. The resulting coordination mode of the ternary complex Cu(II)−GlyGlyHis−Cys differs from that of other peptides, and the less favored formation protects against free radicals as side-products

of the redox reaction. Thus, Cu is transported readily from the albumin model peptide to Cys via the ternary complex and then reduced to Cu(I) [223].

4.6.5. Anticancer Ru(III) complexes in serum

Among the non-platinum tumor-inhibiting agents, two Ru(III) complexes are currently being clinically tested, i.e., imidazolium [*trans*-tetrachloro (dmso)(imidazole) ruthenate(III)] (NAMI-A) (where dmso = dimethyl sulfoxide) and sodium [*trans*-tetrachloridobis(1*H*-indazole)ruthenate(III)] (NKP-1339) (see Fig. 14) [227,228]. The indazolium salt analogue of NKP-1339 (KP1019) is the most promising Ru-based agent and it has completed a phase-I study, although it has low water solubility, which limits the maximum dosage [227,229]. NKP-1339 and NAMI-A are administered intravenously, and they have quite distinct modes of action despite their structural similarities. NKP-1339 is active against solid tumors with minor side effects [227], whereas NAMI-A is directed against the metastasis process with a current focus on lung cancer [228]. These Ru(III) complexes have different hydrolytic properties (aquation and hydrolysis) and binding abilities with serum proteins in terms of the kinetics and thermodynamics of these processes. The rate of aquation (Cl^-/H_2O exchange) of these Ru(III) complexes is affected greatly by the pH, temperature, and the concentrations of chloride and HCO_3^- ions [230, 231], while their redox potentials are in the range of physiological reductants [227]. Thus, aquation and reduction, e.g., by ascorbate, may be possible under the serum conditions, although the binding to serum proteins hinders the efficiency of these processes [231, 232]. In addition, serum protein binding has significant effects on biodistribution, the half-life in the circulation, and clearance, which ultimately affect the pharmacokinetic profile of the drug. Furthermore, HSA and Tf can act as drug carriers (see Section 4.3), thereby justifying further studies of the interactions by NKP-1339 and NAMI-A with these proteins.

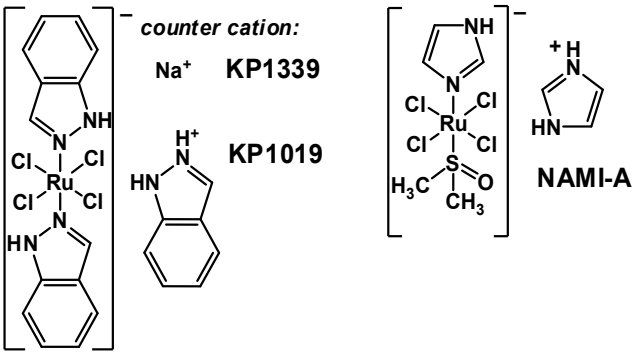

Fig. 14 Chemical structures of Ru(III) complexes in clinical development: NKP-1339 (KP1019) and NAMI-A.

The rapid binding of NKP-1339 to both Tf and HSA has been reported [231-235], although few studies have determined the binding rate constants for the interactions between Ru(III) complexes and proteins. The reaction rates of KP1019 with HSA and apoTf were determined using the CZE–ICP(MS) method ($k_{HSA} = 10.6 \times 10^{-4}$ s^{-1}, $k_{apoTf} = 28.7 \times 10^{-4}$ s^{-1}), which demonstrated the kinetically more favorable binding with apoTf [236]. By contrast the much slower binding of KP1019 with apoTf via covalent bonds was shown by Walsby et al. using EPR spectroscopy [232]. In general, KP1019 and NKP-1339 are described as being bound to HSA in both *in vitro* human serum and *in vivo* samples obtained from treated patients [227,232,236-238, see Fig. 15]. First, the complex NKP-1339 (and KP1019) binds to HSA in a non-covalent manner due to the axial indazole ligand's interaction with the hydrophobic pockets according to EPR measurements [232]. The binding at sites IIA and IIIA has moderate strength ($\log K_{HSA}' = 5.3–5.8$) regardless of the counter-ions, according to combined analyses using ultrafiltration-UV, CZE, and fluorescence spectroscopy (with direct and displacement reactions of the site markers) [233]. However, with longer incubation times, NKP-1339 (and KP1019) is converted into a covalently (coordinatively) bound species. The slow binding of the complex to the side chain donor atoms of HSA via ligand exchange (Cl^-/His nitrogen atoms) may explain the relatively high kinetic inertness of Ru(III) [232]. Therefore, the delivery of NKP-1339 by HSA to cancer cells is assumed to be followed by the enzymatic degradation of HSA and reduction of the Ru(III) complex in the hypoxic environment that is often found in solid tumors because of insufficient tumor vascularization [227]. Reduction leads to the formation of the kinetically more labile Ru(II) complex, which is more capable of reacting with diverse targets (proteins and DNA). The mode of action of NKP-1339 is still unclear, but different factors such as endoplasmic reticulum stress are involved [239].

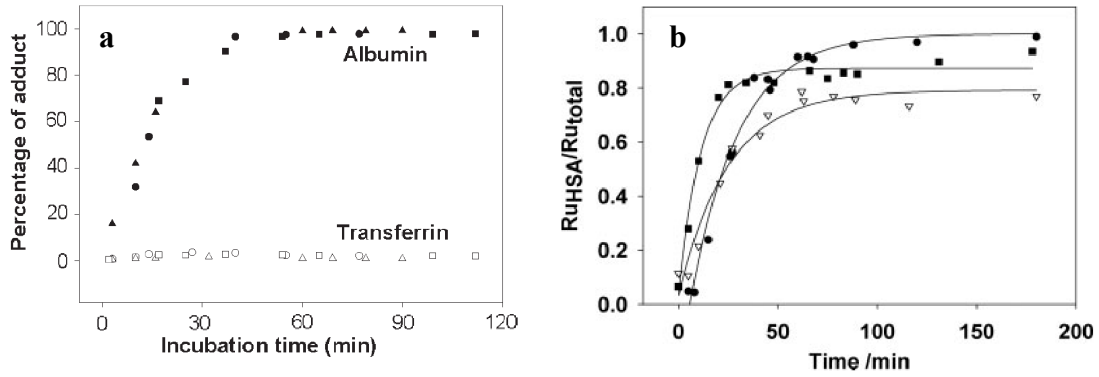

Fig. 15 CE–ICP(MS) monitoring of the binding kinetics for the interaction of KP1019 with HSA and Tf (a). Reproduced from Ref. [236]. Comparison of the *in vitro* binding kinetics of KP1019 with HSA: circles, HSA; triangles, human serum; squares, human plasma (b). Reproduced from Ref. [238].

The coordinating N-donor ligand (indazole) has a prominent role according to the rate and extent of the transport and transformation processes determined for NKP-1339. Modifications of this axial ligand affect numerous properties, such as solubility, lipophilicity, and the ligand exchange rate, as well as the ability to bind to HSA and the redox potential of the complex, where all these factors ultimately influence the bioactivity [240,241].

The kinetic *trans*-effect of the coordinating S-donor dmso ligand in the complex NAMI-A leads to increased lability and a lower redox potential compared with NKP-1339, where these properties make this complex more amenable to hydrolysis and reduction in biological media [231,235,242,243]. NAMI-A also has a high affinity for serum proteins. Rapid binding to Tf was reported by Speiewak et al. because the equilibrium could be reached within 5 min in fluorescence Tyr quenching experiments [234]. Binding constants of $\log K' = 4.11$ [234,244] and 4.01 [234] were determined for apoTf and holoTf, respectively, and coordination at other sites was suggested in addition to the Fe(III) binding sites [234]. Similar to NKP-1339, HSA is also the major binder for NAMI-A in blood serum. EPR experiments by Web et al. [231, 235] indicated rapid binding to HSA in hydrophobic pockets via non-covalent bonds. HSA binding could prevent the reduction of NAMI-A by ascorbate in the serum. The coordination of the His imidazole ligands of the protein was confirmed by ENDOR spectroscopy with a longer incubation time [235].

5. Outlook

Speciation in inert systems refers to the full separation of species and their complete structural identification. This process is entirely different compared with that for labile systems and it involves preparative work, possibly including the application of separation techniques and structural investigation methods in the solid state.

Solution speciation where mostly labile species are in equilibrium with each other and their species distribution is strongly dependent on the experimental conditions is a different issue. The aims of these studies are as follows: (i) obtaining full descriptions of the equilibria, including the distribution of the species in the equilibrium system and determining their characteristics, such as solution structures (binding modes) of the species that are in equilibrium with each other; and (ii) using equilibrium descriptions of these systems in modeling calculations to determine the species distributions of the constituents in conditions where experimental measurements cannot obtain data, e.g., due to extremely low analytical/total concentrations. At present, there is no clear boundary between these two objectives, which may cause difficulties for chemists.

In trace analytical chemistry, speciation is applied widely and it is a rapidly developing area of analytical chemistry. Environmental, medical, and industrial problems will probably force this field to make further improvements in the future, e.g., lowering the detection limits and achieving even better separation of parallel existing species. However, this type of speciation is possible to determine only using certain types of "samples" because *in situ* spectral measurements can only indicate the distribution of one species (or a group of species) or elements on the surface, e.g., complete speciation might not possible in a certain area. For example, fluorescent dyes [245] were developed to detect "free" Cu(I) in cells using a microscope, but no method can determine the complete speciation of copper and measure each of the four species groups at the same time, i.e., the free and bound copper in oxidation states I and II.

Similar to trace analytical speciation, many analytical techniques have been developed to detect different chemical species on surfaces, e.g., X-ray photoelectron spectroscopy, reflection-absorption IR spectroscopy, secondary ion-MS, temperature-programmed techniques, and microscopy techniques such as atomic force microscopy.

As classic studies of complex formation, speciation studies are not "fashionable" at present. For example, the number of annual publications containing pH-potentiometric studies has increased only slightly in recent decades but at a much slower rate than the total number

of coordination chemistry publications [60]. Moreover, these studies are increasingly difficult to publish in highly ranked journals, especially if they are not combined with other methods. The opinion of the scientific community is that speciation can be performed routinely and that stability constant data should be published only in second/third ranked journals. The relatively low "prestige" of these data does not help to improve the reliability of published speciation data. However, reliable and accurate published data are of the utmost importance for any type of chemical project.

Published speciation data are collected in the IUPAC Stability Constants Database [37], which is used mostly by specialists. However, the browsability (e.g., conditional stability constant), parameterization of the speciation calculations (sometimes by hand), and reliability of the data collected in this database should be improved to make it more user-friendly and suitable for a wider range of potential users.

When speciation studies started, potentiometric and photometric studies were the most common techniques, and evaluation programs were designed for these methods. With the exception of HYPERQUAD [246,247], most of these programs are now old-fashioned and not user-friendly. These programs lack input editors, so the input data must be pre-edited and the output is sometimes long and barely understandable to beginners. Graphics are absent or low quality, and the possibilities of modern hardware are not fully utilized. The operation systems used by PCs have changed greatly in the last decades and it may be difficult to even run these programs. The dramatically increased calculation capacity of computer hardware could be applied to automatic model selection and for identifying characteristic errors. In addition, the methods used to calculate the statistical parameters should be reconsidered.

To the best of our knowledge, LAKE [248] is the only program that can handle the dual aspects of NMR spectral data together, i.e., the chemical shift and signal intensity data. The previously mentioned 2D-EPR program is also very inconvenient to operate [63], where the number of components is restricted to only three. No program can handle EPR and UV-Vis data together. Individual evaluations of the data obtained by different methods can yield numerically variant stability data sets, but it is sometimes quite difficult to judge which is more accurate.

Thus, there is a need to develop a user-friendly program that can handle data obtained using different methods (e.g., pH-potentiometry, UV-Vis, CD, and EPR/NMR). The program should be able to evaluate all the input data together to obtain a stability data set, as well as describing EPR/NMR spectra measured according to certain parameters. The low reliably of some published data may be due to the incorrect statistical handling of the measurements.

Therefore, reinterpretations of evaluations and the development of appropriate methods may be necessary to handle data obtained from multiple methods in order to provide correct information about the reliability of the component matrix and the stability constants determined. It would also be useful to assemble the speciation results in a database, including short published data sets as well as all the measurements, evaluations, and statistical parameters, in a similar manner to the Cambridge Structural Database (CSD) [249]. Clearly, determining the basic conditions of such a database is a major undertaking. In particular, many methods are employed for measuring equilibrium data compared with, for example, X-ray studies. Thus, the pH calibration and calculation methods must be unified, or the number of types should be limited, as well as giving full descriptions of them. Initially, it might be easier to handle the data determined by only one method and to classify them based on the technique employed. However, due to the lack of new and publishable data, this database would probably grow quite slowly.

Critical stability constant data compilations based on rigorous selection criteria and expert opinions may provide the stability data needed by non-specialists. These data have been obtained mostly in aqueous solution under normal, everyday conditions. However, there is a great need for stability data obtained in non-aqueous solutions, water-organic solvent mixtures, or unusual experimental conditions (pressure, temperature, or at extremely high concentrations), as well as in the presence of amphipathic molecules or other micelle-forming organic substances, and complex formation processes on the surfaces of solid materials. The latter cases also raise several theoretical issues, which should be clarified. For example, there is no complete description of labile surface processes, probably because the chemical environment of a simple species can be much more complex on the surface compared with that in a dilute solution. A surface does not necessarily have the same environment at every point and a species can have various connections to the surface, especially if the concentration of the species is sufficiently high to form more than one layer. Isotherms are measured routinely to determine the binding capacity of the surface [250], but titrations and kinetic consideration may also be required to determine concentration(s) [250]. Protonation processes [251] and simple complex formation reactions have been quantitatively described [252] on a surface, but few studies have described surface speciation [60].

Other problems include predicting stability data based on theoretical calculations [253], but this appears to be a long process at this stage and it is probably more accurate to estimate a protonation constant [254,255] by selecting one from a database rather than a theoretical calculation.

Simple binary and ternary systems (e.g., the acid-base properties of a compound, or the formation of single ML type complexes with monodentate or bidentate ligands) can be measured easily, but evaluating complex systems (e.g., multidentate ligands form many types of complexes, such as via metal ion hydrolysis or by the formation of protonated complexes to produce quaternary systems) can be difficult even for specialists. Unfortunately, no system is available to address all of these problems. A speciation chemist ideally requires a program that can evaluate the data measurements as well as providing measurement plans based on previous results and giving theoretical predictions. Using the measurements, suggestions can be provided about how to make the experimental details more accurate. However, the community of speciation chemists and the potential users of speciation data might not be sufficiently large as a "market" to invest great efforts in the development of expert computer programs and systems.

Acknowledgements

This study was supported by Hungarian Research Foundation OTKA project PD103905 and the János Bolyai Research Scholarship of the Hungarian Academy of Sciences.

References

[1] D.M. Templeton, F. Arise, R. Cornelis, L-G. Danielsson, H. Muntau, H.P. van Leeuwen, R. Lobinski, Pure Appl. Chem. 72 (2000) 1453.

[2] C.F. Baes, R.E. Mesmer, The Hydrolysis of Cations, Wiley, New York, 1976.

[3] T. Kiss, E. Farkas, in Perspectives on Bioinorganic Chemistry (Eds. R.W. Hay, J.R. Dilworth, K.B. Nolan) Vol. 3, JAI Press, 1996, p. 209.

[4] J.T. Hindmarsh, R.F. McCurdy, CRC Crit. Rev. Clin. Lab. Sci. 23 (1986) 315.

[5] W. Kaim B. Schwederski, Bioinorganic Chemistry: Inorganic Elements in the Chemistry of Life, Wiley, Chichester, 1994.

[6] R. Crichton, Inorganic Biochemistry of Iron Metabolism, Wiley, Chichester, 2001.

[7] J. Buffle, K.J. Wilkinson, M.L. Tercier, N. Partasarathy, in Reviews on Analytical Chemistry, Euroanalysis IX (Eds. F. Palmisano, L. Sabbatini, P.G. Zambonin), Societa Chimica Italiana, 1997.

[8] M.T. Beck, I. Nagypál; Chemistry of Complex Equilibria, Akadémiai kiadó, Budapest, 1990.

[9] J.E. Banks, J. Chem. Educ. 38 (1961) 391.

[10] G. Wilkinson, R. D. Gillard, J. A. McCleverty (Eds.), Comprehensive Coordination Chemistry: The Synthesis, Reactions, Properties & Applications of Coordination Compounds. First ed. Vol. 1. Oxford, England: Pergamon Press, (1987).

[11] A.E. Martell Coordination Chemistry, Vol. 1-2, Von Nostrand Reinhold Co. (1971)/American Chemical Society (1978).

[12] N.N. Greenwood, A. Earnshaw: Chemistry of the Elements, Pergamon Press, Oxford 1984, a: p. 522 b: p. 222.

[13] J. Bjerrum, Metal ammine formation in aqueous solution: theory of the reversible step reactions, P. Haase and Son, Copenhagen, 1941.

[14] M.T. Beck, I. Nagypál; Chemistry of Complex Equilibria, Akadémiai kiadó, Budapest, 1990 a: p.30 b: p. 197 c: p. 141.

[15] I. Sóvágó, D. Sanna, A. Dessi, K. Várnagy, G. Micera, J. Inorg. Biochem. 63 (1996) 99.

[16] F. R. Morral, Alfred Werner and Cobalt Complexes in Advances in Chemistry, American Chemical Society 1967 Vol. 62, Chapter 5, p. 70.

[17] B. N. Figgis, M. A. Hitchman, Ligand Field Theory and its Applications, Whiley, 2000.

[18] H. Yoneda, J. Chrom. 313 (1984) 59.

[19] G. Raj, Advanced Inorganic Chemistry – II 12th edition, KRISHNA Prakashan Media (P) Ltd. India 2010.

[20] I. Nagypál, M.T. Beck, Coord. Chem. Rev. 43 (1982) 233.

[21] L. Alderighi, P. Gans, A. Ienco, D. Peters, A. Sabatinia, A. Vacca, Coord. Chem. Rev. 184 (1999) 311.

[22] I. Puigdomenech, Medusa Chemical Equilibrium Database and Plotting Software (2004) KTH Royal Institute of Technology, www.kth.se/che/medusa.

[23] L. Zékány, I. Nagypál, in: Computational Methods for the Determination of Stability Constants (Ed. D. L. Leggett), Plenum Press, New York, 1985, p. 291.

[24] R. Maggiore, S. Musumeci, S. Sammartano, Talanta 23 (1976) 43.

[25] R.J. Motekaitis, A.E. Martell, Can. J. Chem. 60 (1982) 2403.

[26] A. Bianchi, E. Garcia-España, J. Chem. Educ. 76 (1999) 1727.

[27] P. Letkeman, J. Chem. Educ. 73 (1996) 165.

[28] W.R. Harris, C. Keen, Nutrition, 119 (1989) 1677.

[29] W.R. Harris, Clin. Chem. 39 (1992) 1809.

[30] D.R. Jansena, G.C. Krijgerb, J. Wagenera, R.M. Senwedic, K. Gabanamotsec, M. Kgadietec, Z.I. Kolarb, J.R. Zeevaart, J. Inorg. Biochem. 103 (2009) 1265.

[31] P.M. May in Handbook of Metal Ligand Interactions in Biological Fluids: Bioinorganic Medicine Vol. 2, (Ed. G. Berthon), Marcel Dekker, New York, 1995.

[32] T. Kiss, A. Odani, Bull. Chem. Soc. Jpn., 80, (2007) 1691.

[33] T. Jakusch, D. Hollender, É.A. Enyedy, C. S. González, M. Montes-Bayón, A. Sanz-Medel, J. Costa Pessoa, I. Tomaz, T. Kiss, Dalton Trans. (2009) 2428.

[34] A.K. Bytzek, É.A. Enyedy, T. Kiss, B.K. Keppler. C.G. Hartinger, Electrophoresis, 30 (2008) 4075.

[35] E.A. Enyedy, O. Dömötör, K. Bali, A. Hetényi, T. Tuccinardi, B.K. Keppler, J. Biol. Inorg. Chem. 20 (2015) 77.

[36] G.E. Jackson, M.J. Byrne, J. Nucl. Med. 37 (1996) 379.

[37] SCQuery, The IUPAC Stability Constants Database, Academic Software (Version 5.5), Royal Society of Chemistry, 1993–2005.

[38] P. Debye, E. Hückel, Physik. Z. 24 (1923) 185.

[39] K.S. Pitzer, Activity coefficients in electrolyte solutions (2nd ed.). Boca Raton, CRC Press, 1991.

[40] C.W. Davies, J. Chem. Soc. (1938) 2093.

[41] G. Schwarzenbach, G. Anderegg, Helv. Chim. Acta 40 (1957) 1773.

[42] G. Peintler, I. Nagypál, A. Jancsó, I. R. Epstein, K. Kustin, J. Phys. Chem. A, 101, (1997) 8013.

[43] E.A. Enyedy, O. Dömötör, E. Varga, T. Kiss, R. Trondl, C.G. Hartinger, B.K. Keppler, J. Inorg. Biochem. 117 (2012) 189.

[44] I. Correia, J. Costa Pessoa, M.T. Duarte, R.T. Henriques, M.F.M. Piedade, L.F. Veiros, T. Jakusch, T. Kiss, Á. Dörnyei, M.M.C. A. Castro, C.F. G.C. Geraldes, F. Avecilla, Chem. Eur. J. 10 (2004) 2301.

[45] B. Noszál, J. Phys. Chem. 90 (1986) 6345.

[46] B. Noszál, Magy. Kém. Foly. 87 (1981) 168.

[47] E.I. Solomon, A.B.P. Lever, Inorganic electronic structure and spectroscopy, Wiley-Interscience, 2006, p. 78.

[48] K. Ősz, B. Bóka, K. Várnagy, I. Sóvágó, T. Kurtan, S. Antus, Polyhedron 21 (2002) 2149.

[49] H. Sigel, R.B. Martin, Chem. Rev. 82 (1982) 385.

[50] F.S. Richardson, J. Chem. Phys. 54 (1971) 2453.

[51] J.R. Lakowicz, Principles of Fluorescence Spectroscopy, 3rd ed., Springer, Singapure, 2006.

[52] F.H. Köhler, Paramagnetic Complexes in Solution: The NMR Approach. eMagRes., John Wiley, 2011.

[53] S.J. Peters, C.D. Stevenson, J. Chem. Educ. 81 (2004) 715.

[54] A.D. Gift, S.M. Stewart, P.K. Bokashanga, J. Chem. Educ. 89 (2012) 1458.

[55] R. Tribolet, R.B. Martin, H. Sigel, Inorg. Chem. 26 (1987) 638.

[56] Z. Nagy, I. Sóvágó, J. Chem. Soc., Dalton Trans. (2001) 2467.

[57] É.A. Enyedy, É. Sija, T. Jakusch, C.G. Hartinger, W. Kandioller, B.K. Keppler, T. Kiss, J. Inorg. Biochem. 127 (2013) 161.

[58] L. Pettersson, K. Elvingson, ACS Symposium Series, 711(Vanadium Compounds) (1998) 30.

[59] A. Gorzsás, I. Andersson, L. Pettersson, J. Inorg. Biochem. 103 (2009) 517.

[60] SciFinder Scholar, version 2016; Chemical Abstracts Service: Columbus, OH, 2016.

[61] W.E. Blumberg, J. Peisach, Life Chemistry Reports, 5 (1987) 5.

[62] T.S. Smith, R. LoBrutto, V.L. Pecoraro, Coord. Chem. Rev. 228 (2002) 1.

[63] A. Rockenbauer, T. Szabó-Plánka, Z. Árkosi, L. Korecz, J. Am. Chem. Soc. 123 (2001) 7646.

[64] V.B. Di Marco, G.G. Bombi, Mass Spec. Rev. 25 (2006) 347.

[65] L.W. McDonald, J. A. Campbell, S. B. Clark, Anal. Chem. 86 (2014) 1023.

[66] G. Berthon, Handbook of Metal Ligand Interactions in Biological Fluids, Volumes 1–4, Marcel Dekker, New York, 1995.

[67] A. Ure, C. Davidson, Chemical Speciation in the Environment, Blackwell, Oxford, 2002.

[68] T. Jakusch, J. Costa Pessoa, T. Kiss, Coord. Chem. Rev. 255 (2011) 2218.

[69] D. Sanna, G. Micera, E. Garriba, Inorg. Chem. 49 (2010) 174.

[70] T. Kiss, T. Jakusch, D. Hollender, É.A. Enyedy, L. Horváth, J. Inorg. Biochem. 103 (2009) 527.

[71] W.H. Schroeder, Trends Anal. Chem. 8 (1989) 339.

[72] O. Lindquist, H. Rodhe, Tellus 37B, (1985) 136.

[73] E. Yildirim; L. S. Yildirim, in Speciation Studies in Soil, Sediment and Environmental Samples, (Ed. S. Bakirdere), CRC Press, 2014, p. 1.

[74] A. Kot-Wasik, J. Namieśnik, Trends Anal. Chem. 19 (2000) 69.

[75] H. Tang, F. Xiao, D. Wang, Adv. Colloid Interface Sci. Part A 226 (2015) 78.

[76] R.S. Multani, T. Feldmann, G.P. Demopoulos, Hydrometallurgy 164 (2016) 141.

[77] G. Ungureanu, S. Santos, R. Boaventura, C. Botelho, J. Environ. Manage. 151 (2015) 326.

[78] C.G. Sartal, M.C.B. Alonso, B. Barciela; Barrera, in Seafood Science (Ed. S.-K. Kim), CRC Press, 2015 p. 276.

[79] D. Sanchez-Rodas, A.M. Sanchez de la Campa, L. Alsioufi, Anal. Chim. Acta 898 (2015) 1.

[80] T. Yoneyama, S. Ishikawa, S. Fujimaki, Int. J. Mol. Sci. 16 (2015) 19111.

[81] V. Kumar, A.K. Chopra, World App. Sci. J. 33 (2015) 944.

[82] B. Markiewicz, I. Komorowicz, A. Sajnóg, M. Belter, D. Barałkiewicz, Talanta 132 (2015) 814.

[83] S. Chakraborty, P. Chakraborty, B.N. Nath, Mar. Pollut. Bull. 97 (2015) 36.

[84] L. Zhang, S. Wang, Q. Wu, F. Wang, C.J. Lin, L. Zhang, M. Hui, M. Yang, H. Su, J. Hao, Atm. Chem. Phys. 16 (2016) 2417.

[85] A.T. Reis, C.M. Davidson, C. Vale, E. Pereira, TrEAC-Trend. Anal. Chem. 82 (2016) 109.

[86] S.-W. Lee, G.V. Lowry, H. Hsu-Kim, Environ. Sci. Proc. Imp. 18 (2016) 176.

[87] M. Pettine, T.J. McDonald, M. Sohn, G.A.K. Anquandah, R. Zboril, V.K. Sharma, TrEAC-Trend. Anal. Chem. 5 (2015) 1.

[88] S. Sindern, J. Schwarzbauer, L. Gronen, A. Goertz, S. Heister, M. Bruchmann, Int. J. Environ. Anal. Chem. 95 (2015)790.

[89] N. Belzile, Y-W. Chen, Appl. Geochem. 63 (2015) 83.

[90] F. Endrizzi, C.J. Leggett, L. Rao, Ind. Eng. Chem. Res. 55 (2016) 4249.

[91] T. Yoneyama, S. Ishikawa, S. Fujimaki, Int. J. Mol. Sci. 16 (2015) 19111.

[92] M. Leermakers, W. Baeyens, P. Quevauviller, M. Horvat, Trends Anal. Chem. 24 (2005) 383.

[93] M. Amde, Y. Yin, D. Zhang, J. Liu, Chem. Spec. Bioavailab. 28 (2016) 51.

[94] J. Ščančar, R. Milačič, Anal. Bioanal. Chem. 386 (2006) 999.

[95] K. Pyrzyfiska, Mikrochim. Acta 122 (1996) 279.

[96] W.R. Cullen, K.J. Reimer, Chem. Rev. 89 (1989) 713.

[97] R. Rakhunde, L. Deshpande, H.D. Juneja, Crit. Rev. Env. Sci. Tech. 42 (2012) 776.

[98] B. Salbu, Speciation: Radionuclides. Encyclopedia of Inorganic and Bioinorganic Chemistry, John Wiley and Sons, 2011.

[99] Ph. Quevauviller, in Chemical Speciation in the Environment, (Eds. A. M. Ure, C.M. Davidson), Blackwell Science Ltd, Oxford, 2002, p. 146.

[100] M. Filella, R.M. Town, J. Buffle, in Chemical Speciation in the Environment (Eds. A. M. Ure, C.M. Davidson), Blackwell Science Ltd, Oxford, 2002, p. 188.

[101] R.H. Byrne, in Chemical Speciation in the Environment (Eds. A. M. Ure, C.M. Davidson), Blackwell Science Ltd, Oxford, 2002, p. 322.

[102] P.H.E. Gardiner, in Chemical Speciation in the Environment (Eds. A. M. Ure, C.M. Davidson), Blackwell Science Ltd, Oxford, 2002, p. 387.

[103] P. Apostoli, R. Cornelis, J. Duffus, P. Hoet, D. Lison, D. Templeton, Elemental Speciation in Human Health Risk Assessment, WHO, Environmental Health Criteria 234, 2006.

[104] K.J. Powell, P.L. Brown, R.H. Byrne, T. Gajda, G. Hefter, A-K. Leuz, S. Sjöberg, H. Wanner, Pure Appl. Chem. 85 (2013) 2249.

[105] D.G. Lumsdon, L.J. Evans, in Chemical Speciation in the Environment, Eds. A. M. Ure, C.M. Davidson, Blackwell Science Ltd, Oxford, 2002, p. 89.

[106] A.E. Martell, R.M. Smith, R.J. Rotekaitis, NIST Critically Selected Stability Constants of Metal Complexes Database. National Institute of Standards and Technology, Gaithersburg, 2003

[107] P.M. May, K. Murray, J. Chem. Eng. Data 46 (2001) 1035.

[108] A.M.M. Leal, M.J. Blunt, T.C. LaForce, Geochim. Cosmochim. Acta 131 (2014) 301.

[109] D. Rowland, P.M. May, Talanta 81 (2010) 149.

[110] J.D. Allison, D.S. Brown, K.J. Novo-Gradac, MINTEQA2/PRODEFA2--A geochemical assessment model for environmental systems--Version 3.0 user's manual: Athens, Georgia, Environmental Research Laboratory, Office of Research and Development, U.S. Environmental Protection Agency, 1990, p 106.

[111] J.W. Akitt, J.M. Eldrers, J. Chem. Soc. Dalton Trans. (1988) 1347.

[112] L.M. Hyman, K.J. Franz, Coord. Chem. Rev. 256 (2012) 2333.

[113] J.M. Harrington, T. Gootz, M. Flanagan, M. Lall, J. O'Donnell, J. Winton, J. Muellel, A.L. Crumbliss, Biometals, 25 (2012) 1023.

[114] G. Lente, I. Fábián, Inorg. Chem., 38 (1999) 603.

[115] A. Stefansson, Environ. Sci. Technol. 41 (2007) 6117.

[116] D.C. Crans, K.A. Woll, K. Prusinskas, D. Johnson, E. Norkus, Inorg. Chem. 52 (2013) 12262.

[117] W. Schneider, Comments Inorg. Chem. 5 (1984) 205.

[118] A.K. Powell in Met. Ions in Biol Syst. 35 (1998) 515.

[119] T. Peters Jr, All About Albumin: Biochemistry, Genetics, and Medical Applications, Academic Press, San Diego, CA, 1996.

[120] M.L. Bishop, E.P. Fody, L.E. Schoeff (Eds.) Clinical Chemistry: Principles, Techniques, and Correlations, Wolters Kluwer, 2013.

[121] G. Fanali, A. Masi, V. Trezza, M. Marino, M. Fasano, P. Ascenzi, Mol. Aspects Med. 33 (2012) 209.

[122] W. Bal, M. Sokołowska, E. Kurowska, P. Faller, Biochim. Biophys. Acta 1830 (2013) 5444.

[123] C.A. Blindauer, J. Lu, A. J. Stewart, P.J. Sadler, T.J.T. Pinheiro, Biochem. Soc. Trans. 36 (2008) 1317.

[124] W. Bal, J. Christodoulou, P.J. Sadler and A. Tucker, J. Inorg. Biochem. 70 (1998) 33.

[125] P.J. Sadler, A.J. Stewart, C.A. Blindauer, S. Berezenko, D. Sleep, Proc. Natl. Acad. Sci. U. S. A. 100 (2003) 3701.

[126] R.R. Crichton, M. Charloteaux-Wauters, FEBS 164 (1987) 485.

[127] S. Bailey, R.W. Evans, R.C. Garratt, B. Gorinsky, H. Samar, C. Christopher, H. Jhoti, P.F. Lindley, A. Mydin, Assanah, R. Sarra, J.L. Watson, Biochemistry 27 (1988) 5804.

[128] H. Sun, H. Li, P.J. Sadler, Chem. Rev. 99 (1999) 2817.

[129] Harrison's Principles of Internal Medicine, 17th ed., McGraw-Hill Education, 2008, p. 2432 (Table 351-2).

[130] J.B. Vincent, S. Love, Biochim. Biophys. Acta 1820 (2012) 362.

[131] A. Gonzalez-Quintela, R. Alende, F. Gude, J. Campos, J Rey, L.M. Meijide, C. Fernandez-Merino, C. Vidal, Clin. Exp. Immunol. 151 (2008) 42.

[132] A.A. Rehman, H. Ahsan, F.H. Khan, Cell. Physiol. 228 (2013) 1665.

[133] T. Kiss, J. Inorg. Biochem. 128 (2013) 156.

[134] W.R. Harris, Z. Wang, Y.Z. Hamada, Inorg. Chem. 42, (2003) 3262.

[135] A.B. S. Cabezuelo, E.B. Gonzales, J.I.G. Alomso, A. Sanz-Medel, Analyst 123 (1998) 865.

[136] K. Atkári, T. Kiss, R. Bertani, R.B. Martin, Inorg. Chem. 1996, 35, 7089.

[137] IDF Diabetes Atlas 7th ed., International Diabetes Federation. 2015, p. 13.

[138] Williams Textbook of Endocrinology (12th ed.). Elsevier/Saunders, Philadelphia p. 1371.

[139] J. H. Koeslag, P. T. Saunders, E. Terblanche (June 2003), The Journal of Physiology (2003) 549 (Pt 2): 333–46.

[140] H. Sakurai, Y. Kojima, Y. Yoshikawa, K. Kawabe, H. Yasui, Coord. Chem. Rev. 226 (2002) 187.

[141] J. Fugono, K. Fujimoto, H. Yasui, K. Kawabe, Y. Yoshikawa, Y. Kojima, H. Sakurai, Drug Metabol. Pharmacokinet. 17 (2002) 340).

[142] C.E. Heyliger, A.G. Tahiliani, J. H. McNeill, Science 227 (1985) 1474.

[143] D. Rehder; J. Costa Pessoa, C.F.G.C. Geraldes, M.M.C.A. Castro, T. Kabanos, T. Kiss, B. Meier, G. Micera, L. Pettersson, M. Rangel, A. Salifoglou, I. Turel, D. Wang, J. Biol. Inorg. Chem. 7 (2002) 384.

[144] H. Sakurai, J. Fugono, H. Yasui, Mini-Rev. Med. Chem. 4 (2004) 41.

[145] T. Kiss, E. Kiss, G. Micera, D. Sanna, Inorg. Chim. Acta 283 (1998) 202.

[146] E. Kiss, E. Garribba, G. Micera, T. Kiss, H. Sakurai, J. Inorg. Biochem. 78 (2000) 97.

[147] T. Kiss, E. Kiss, E. Garribba, H. Sakurai, J. Inorg. Biochem. 80 (2000) 65.

[148] P. Buglyó, E. Kiss, I. Fábián, Inorg. Chim. Acta 306 (2000) 174.

[149] P. Buglyó, T. Kiss, E. Kiss, D. Sanna, E. Garribba, G. Micera, J. Chem. Soc., Dalton Trans. (2002) 2275.

[150] E. Kiss, K. Kawabe, A. Tamura, T. Jakusch, H. Sakurai, T. Kiss, J. Inorg. Biochem. 95 (2003) 69.

[151] H. Sakurai, A. Tamura, J. Fugano, H. Yasui, T. Kiss, Coord. Chem. Rev. 245 (2003) 31.

[152] T. Jakusch, A. Dean, T. Oncsik, A.C. Bényei, V. Di Marco, T. Kiss, Dalton Trans. (2010) 212.

[153] A. Gorzsás, I. Andersson, L. Pettersson, Eur. J. Inorg. Chem. (2006) 3559.

[154] E. A. Enyedy, L. Horváth, K. Gajda-Schrantz, G. Galbács, T. Kiss, J. Inorg. Biochem. 100 (2006) 1936.

[155] D. Sanna, P. Buglyó, G. Micera, E. Garribba, J. Biol. Inorg. Chem. 15 (2010) 825.

[156] E. Garribba, D. Sanna, G. Micera, J. Inorg. Biochem. 2009, 103, 648.

[157] I. Correia, T. Jakusch, E. Cobbinna, S. Mehtab, I. Tomaz, N.V. Nagy, A. Rockenbauer, J. Costa Pessoa, T. Kiss, Dalton Trans. 41 (2012) 6477.

[158] D. Sanna, G. Micera, E. Garribba, Inorg. Chem. 50 (2011) 3717.

[159] T. Kiss, T. Jakusch, B. Gyurcsik, A. Lakatos, É.A. Enyedy, É. Sija, Coord. Chem. Rev. 256 (2012) 125.

[160] T. Kiss, T. Jakusch, S. Bouhsina, H. Sakurai, É.A. Enyedy, Eur. J. Inorg. Chem. (2006) 3607.

[161] K.H. Thompson, B.D. Liboiron, Y. Sun, K.D.D. Bellman, I.A. Setyawati, B.O. Patrick, V. Karunaratne, G. Rawji, J. Wheeler, K. Sutton, S. Bhanot, C. Cassidy, J.H. McNeill, V.G. Yuen, C. Orvig, J. Biol. Inorg. Chem. 8 (2003) 66.

[162] A. Levina, A.I. McLeod, S.J. Gasparini, A. Nguyen, W.G.M. De Silva, J.B. Aitken, H.H. Harris, C. Glover, B. Johannessen, P. Lay, Inorg. Chem. 54 (2015), 7753.

[163] G.R. Willsky, L.-H. Chi, M. Godzala III, P.J. Kostyniak, J.J. Smee, A.M. Trujillo, J.A. Alfano, W. Ding, Z. Hu, D.C. Crans, Coord. Chem. Rev. 255 (2011) 2258.

[164] A.G. Sostarecz, E. Gaidamauskas, S. Distin, S.J. Bonetti, N.E. Levinger, D.C. Crans, Chem. A Eur. J. 20 (2014) 5149.

[165] D.C. Crans, L. Yang, T. Jakusch, T. Kiss, Inorg. Chem. 39 (2000) 4409.

[166] J. Masouka, P. Saltman, J. Biol. Chem. 269 (1994) 25557.

[167] A.J. Stewart, C.A. Blindauer, S. Berezenko, D. Sleep, P.J. Sadler, Proc. Natl. Acad. Sci. U.S.A. 100 (2003) 3701.

[168] N.F. Adham, M.K. Song, H. Rinderknecht, Biochim. Biophys. Acta Protein Struct. 495 (1977) 212.

[169] S. Killerich, C. Christiansen, Clin. Chim. Acta 154 (1986) 1.

[170] J.D. Boyett, J.F. Sullivan, Metab. Clin. Exp. 19 (1970) 148.
[171] J.W. Foote, H.T. Delves, J. Clin. Pathol. 37 (1984) 1050.
[172] W.R. Harris, Biochemistry 22 (1983) 3920.
[173] P.A. Charlwood, Biochim. Biophys. Acta Protein Struct. 581 (1979) 260.
[174] Y.-R. Zheng, K. Suntharalingam, T.C. Johnstone, H. Yoo, W. Lin, J.G. Brooks, S.J. Lippard, J. Am. Chem. Soc. 136 (2014) 8790.
[175] F. Kratz, R. Müller-Driver, I. Hofmann, J. Drevs, C.J. Unger, Med. Chem. 43 (2000) 1253.
[176] F. Liu, J. Mu, B. Xing, Curr. Pharm. Des. 21 (2015) 1866.
[177] V. Pichler, J. Mayr, P. Heffeter, O. Dömötör, É.A. Enyedy, G. Hermann, D. Groza, G. Köllensperger, M. Galanksi, W. Berger, B.K. Keppler, C.R. Kowol, Chem. Commun. 49 (2013) 2249.
[178] A.R. Timerbaev, C.G. Hartinger, S.S. Aleksenko, B.K. Keppler, Chem Rev. 106 (2006) 2224.
[179] H. Holtkamp, G. Grabmann, C.G. Hartinger, Electrophoresis 37 (2016) 959.
[180] B. Michalke, J. Trace Elem. Med. Biol. 24 (2010) 69.
[181] M.A. Graham, G.F. Lockwood, D. Greenslade, S. Brienza, M. Bayssas, E. Gamelin, Clin. Cancer Res. 6 (2000) 1205.
[182] A.V. Rudnev, S.S. Aleksenko, O. Semenova, C.G. Hartinger, A.R. Timerbaev, B.K. Keppler, J. Sep. Sci. 28 (2005) 121.
[183] A.I. Ivanov, J. Christodoulou, J.A. Parkinson, K.J. Barnham, A. Tucker, J. Woodrowi, P.J. Sadler, J. Biol. Chem. 273 (1998) 14721.
[184] X-Ray CE Course - Radiography of the Upper Extremities, ebook, 2015 CE4RT.com Las Vegas.
[185] C.F.G.C. Geraldes, S. Laurent, Contrast Media Mol. Imaging 4 (2009) 1.
[186] C.S. Bonnet, É. Tóth, in Ligand Design in Medicinal Inorganic Chemistry, 1st ed. (Ed. Tim Storr) Wiley, 2014, p. 321.
[187] B. Drahos, I. Lukes, E. Tóth, J. Inorg. Chem. 2012 (2012) 1975.
[188] C.H. Evans, Biochemistry of the Lanthanides, Plenum, New York, 1990, p. 25.
[189] P. Caravan, J.J. Ellison, T.J. McMurry, R.B. Lauffer, Chem. Rev. 99 (1999) 2293.
[190] E. Brücher, G. Tircsó, Z. Baranyai, Z. Kovács, A.D. Sherry, in The Chemistry of Contrast Agents in Medical Magnetic Resonance Imaging, 2nd ed. (Eds: A. E. Merbach, L. Helm, E. Tóth), Wiley, Chichester (UK), 2013, p. 157.
[191] T. Grobner, Nephrol. Dial. Transplant. 21 (2005) 1104.

[192] P. Marckmann, L. Skov, K. Rossen, A. Dupont, M.B. Damholt, J.G. Heaf, H.S. Thomsen, J. Am. Soc. Nephrol. 17 (2006) 2359.

[193] M.A. Perazella, R.A. Rodby, Seminars in Dialysis 20 (2007) 179.

[194] J.G. Penfield, R.F. Reilly, Nat. Clin. Pract. Nephrol. 3 (2007) 654.

[195] S. K. Morcos, Br. J. Radiol. 80 (2007) 73.

[196] C. Thakral, J. Alhariri, J. L. Abraham, Contrast Media Mol. Imaging 2 (2007) 199.

[197] P. Marckmann, L. Skov, K. Rossen, J. G. Heaf, H. S. Thomsen, Nephrol. Dial. Transplant. 22 (2007) 3174.

[198] E. A. Sadowski, L. K. Bennett, M. R. Chan, A. L. Wentland, A. L. Garrett, R. W. Garrett, A. Djamali, Radiology 243 (2007) 148.

[199] Y. B. Wang, T. K. Alkasab, O. Narin, R. M. Nazarian, R. Kaewlai, J. Kay, H. H. Abujudeh, Radiology 260 (2011) 105.

[200] K. Kitajima, T. Maeda, S. Watanabe, Y. Ueno, K. Sugimura, Int. J. Urol. 19 (2012) 1127.

[201] G. Bongartz, Magn. Reson. Mater. Phys. Biol. Med. 20 (2007) 57.

[202] R. F. Reilly, Clin. J. Am. Soc. Nephrol. 3 (2008) 747.

[203] H. Wollanka, W. Weidenmaier, C. Giersig, Nephrol. Dial. Transplant. 24 (2009) 3882.

[204] T. Collidge, P. Thomson, P. Mark, W. Willinek, G. Roditi, Nephrol. Dial. Transplant. 25 (2010) 1352.

[205] T. R. Elmholdt, B. Jorgensen, M. Ramsing, M. Pedersen, A. B. Olesen, Clin. Kidney J. 3 (2010) 285.

[206] Z. Baranyai, E. Brücher, F. Uggeri, A. Maiocchi, I. Tóth, M. Andrási, A. Gáspár, L. Zékány, S. Aime, Chem. Eur. J. 21 (2015) 4789.

[207] M. Matzapetakis, M. Kourgiantakis, M. Dakanali, C.P. Raptopoulu, A. Terzis, A. lakatos, T. Kiss, I. Bányai, L. Ioranidis, T. Mavromoustakos, A. Salifoglou, Inorg. Chem. 40 (2001) 1734.

[208] A. Lakatos, F. Evanics, G. Dombi, R. Bertani, T. Kiss, Eur. J. Inorg. Chem. (2001) 3079.

[209] J.D. Bell, G. Kubal, S. Radulovic, P. Sadler, A. Tucker, Analyst 118, (1993) 241.

[210] T. Bantam, R. Milacic, B. Mitrovic, B. Pihlar, J. Anal. At. Spectrom. 14, (1999) 1743.

[211] J. Beardmore, C. Exley, J. Inorg. Biochem. 103, (2003) 205–209.

[212] D.R. Williams, C.C. Combes, L. Wu, in Handbook of Metal-Ligand Interactions in Biological Fluids: Bioinorganic Medicine, Vol. 2, Part V, (Ed. G. Berthon), Marcel Dekker, New York, 1995, p. 1195.

[213] M. E. J. Curzon, T. W. Cutress, Trace Elements and Dental Diseases, Wright PSG, Bristol, 983, p 110.

[214] D. R. Williams, L. Wu,Chem. Speciation Bioavailability 5 (1993) 107.

[215] Z. Nagy, I. Fábián, I. Sóvágó, J. Inorg. Biochem. 79 (2000) 129.

[216] C.D.W. Fröhlig, W.S. Sheldrick, J. Chem. Soc., Chem. Commun. (1997) 1737.

[217] D. Wolters, W.S. Sheldrick, J. Chem. Soc., Dalton Trans. (1999) 1121.

[218] M. Hahn, D. Wolters, W.S. Sheldrick, F.B. Hulsbergen, J. Reedijk, J. Biol. Inorg. Chem. 4 (1999) 412.

[219] B. Sarkar, T.P.A. Kruck, in Biochemistry of Copper, (Eds. J. Peisach, P. Aissen, W.E. Blumberg), Academic Press, New York, 1966, p. 183.

[220] M.C. Linder, N.A. Lomeli, S. Donley, F. Mehrbod, P. Cerveza, S. Cotton, L. Wooten, Copper Transport and its Disorders in Experimental Medicine and Biology Vol.448 (Eds: A. Leone, J.F.B. Mercer), Academic/Plenum, New York, 1999, p. 1.

[221] P.Z. Naumann, A. Saas-Kortsak, J. Clin. Invest. 46 (1967) 646.

[222] B. Sarkar, Chem. Rev. 99 (1999) 2535.

[223] P. Deschamps, P.P. Kulkarni, M. Gautam-Basak, B. Sarkar, Coord. Chem. Rev. 249 (2005) 895.

[224] A. Hanaki, Y. Funahashi, A. Odani, J. Inorg. Biochem. 100 (2006) 305.

[225] R.A. Lovstad, BioMetals 15 (2002) 351–359.

[226] A. Hanaki, N. Ikota, J. Ueda, T. Ozawa, A. Odani, Bull. Chem. Soc. Jpn. 76 (2003) 2143.

[227] R. Trondl, P. Heffeter, C.R. Kowol, M.A. Jakupec, W. Berger, B.K. Keppler, Chem. Sci. 5 (2014) 2925.

[228] A. Bergamo, C. Gaiddon, J.H.M. Schellens, J.H. Beijnen, G. Sava, J. Inorg. Biochem. 106 (2012) 90.

[229] C.G. Hartinger, M.A. Jakupec, S. Zorbas-Seifried, M. Groessl, A. Egger, W. Berger, H. Zorbas, P.J. Dyson, B.K. Keppler, Chem. Biodivers. 5 (2008) 2140.

[230] A. Kung, T. Pieper, R. Wissiack, E. Rosenberg, B.K. Keppler, J. Biol. Inorg. Chem. 6 (2001) 292.

[231] M.I. Webb, C.J. Walsby, Dalton Trans. 40 (2011) 1322.

[232] N. Cetinbas, M.I. Webb, J.A. Dubland, C.J. Walsby, J. Biol. Inorg. Chem. 15 (2010) 131.

[233] O. Dömötör, C.G. Hartinger, A.K. Bytzek, T. Kiss, B.K. Keppler, E.A. Enyedy, J. Biol. Inorg. Chem. 18 (2013) 9.

[234] K. Śpiewak, M. Brindell, J. Biol. Inorg. Chem. 20 (2015) 695.

[235] M.I. Webb, C.J. Walsby, Dalton Trans. 44 (2015) 17482.

[236] K. Polec-Pawlak, J.K. Abramski, O. Semenova, C.G. Hartinger, A.R. Timerbaev, B.K. Keppler, M. Jarosz, Electrophoresis 27 (2006) 1128.

[237] M. Sulyok, S. Hann, C.G. Hartinger, B.K. Keppler, G. Stingeder, G. Koellensperger, J. Anal. At. Spectrom. 20 (2005) 856.

[238] M. Groessl, C.G. Hartinger, K. Polec-Pawlak, M. Jarosz, B.K. Keppler, Electrophoresis 29 (2008) 2224.

[239] L.S. Flocke, R. Trondl, M.A. Jakupec, B.K. Keppler, Invest. New Drugs. 34 (2016) 261.

[240] S.W. Chang, A.R. Lewis, K.E. Prosser, J.R. Thompson, M. Gladkikh, M.B. Bally, J.J. Warren, C.J. Walsby, Inorg. Chem. 55 (2016) 4850.

[241] P.-S. Kuhn, V. Pichler, A. Roller, M. Hejl, M.A. Jakupec, W. Kandioller, B.K. Keppler, Dalton Trans. 44 (2015) 659.

[242] M. Bouma, B. Nuijen, M.T. Jansen, G. Sava, A. Flaibani, A. Bult, J.H. Beijnen, Int. J. Pharm. 248 (2002) 239.

[243] M. Brindell, D. Piotrowska, A.A. Shoukry, G. Stochel, R.van Eldik, J. Biol. Inorg. Chem. 12 (2007) 809.

[244] O. Mazuryk, K. Kurpiewska, K. Lewiński, G. Stochel, M. Brindell, J. Inorg. Biochem. 116 (2012) 11.

[245] C. Shen, E.J. New, Metallomics 7 (2015) 56.

[246] Hyperquad2013, Equilibrium Constants from Potentiometric Data, © 2013 Protonic Software.

[247] P. Gans, A. Sabatini, A. Vacca, Talanta, 43 (1996) 1739.

[248] N. Ingri, I. Andersson, L. Pettersson, A. Yagasaki, L. Andersson, K. Holmström, Acta Chem. Scand. 50, 1996 717.

[249] Cambridge Structural Database (CSD), Cambridge Crystallographic Data Centre (CCDC), http://www.ccdc.cam.ac.uk/.

[250] Suarez, D. L.; Goldberg, S.; Su, C. From ACS Symposium Series (1998), 715(Mineral-Water Interfacial Reactions), 136–178.

[251] T. de F. Paulo, H.D. Abruna, I.C.N. Diogenes, Langmuir 28 (2012) 17825.

[252] P.W. Schindler, in Metal Ions in Biological Systems 18 (1984) 105.

[253] O. Gutten, L. Rulisek, Inorg. Chem. 52 (2013) 10347.

[254] I.E. Charif, S.M. Mekelleche, D. Villemin, N. Mora-Diez, J. Mol. Struct.: Theochem 818 (2007) 1.
[255] F. Yao, W. Hua-Jing, C. Sha-Sha, G. Qing-Xiang, L. Lei, J. Org. Chem. 74 (2009) 810.

Abbreviations

α2M	alpha-2-macroglobulin
AA	amino acid
acac	acetylacetone
AcMet	acetyl-methionine
apoTf	apotransferrin
ATCUN	amino terminal Cu(II) and Ni(II) binding side
BMA	*bis*-(methylamide)
CD	circular dichroism
CP	calcium hydrogenphosphate
cyt	cytidine
CZE	capillary zone electrophoresis
CZE-ICP-MS	capillary zone electrophoresis inductively coupled plasma mass spectrometry
dhp	1,2 dimethyl-3-hydroxy-4-pyridinone
dien	diethylenetriamine
DM	Diabetes mellitus
dmso	dimethyl sulfoxide
DNA	deoxyribonucleic acid
DOTA	tetraazacyclododecane-1,4,7,10-tetraacetic acid
DTPA	diethylenetriaminepentaacetic acid
DTPA-BMA	1,7-Bis(methylcarbamoylmethyl)-1,4,7-triazaheptane-1,4,7-triacetic acid
ENDOR	electron nuclear double resonance
EPR	electron paramagnetic resonance
ESI-MS	electrospray ionization-mass spectrometry
FAP	fluoroapatite
GaM	*tris(maltolato)*gallium(III)
GSH	glutathione
GI	gastrointestinal
HAP	hydroxyapatite
HMM	high molecular mass
HPLC	high-performance liquid chromatography
hpno	2-hydroxypyridine 1-oxide
HSA	human serum albumin
ICP-MS	inductively coupled plasma-mass spectrometry
Ig	Immunoglobulin
IUPAC	International Union of Pure and Applied Chemistry
KP1019	indazolium [*trans*-tetrachloridobis(1*H*-indazole)ruthenate(III)]
KP46	*tris*(8-quinolinolato)gallium(III)
L	ligand of any kind in the fully deprotonated form; charge is usually omitted for simplicity
LMM	low molecular mass
M	metal ion; charge is usually omitted for simplicity
mal	maltol
MRI	magnetic resonance imaging
MS	mass spectrometry
nta	nitrilotriacetic acid
NAMI-A	imidazolium [*trans*-tetrachloro(dmso)(imidazole)ruthenate(III)]
NKP-1339	sodium [*trans*-tetrachloridobis(1*H*-indazole)ruthenate(III)]

NMG	*N*-methyl-glucosamine
NMR	nuclear magnetic resonance
NSF	nephrogenic systemic fibrosis
pic	picolinic acid
TCP	tricalcium phosphate
terpy	terpyridine
Tf	human serum transferrin
UV-Vis	UV-visible
XANES	X-ray absorption near edge structure